AD-A064 369 AIR FORCE INST OF TECH WRIGHT-PATTERSON AFB OHIO SCH--ETC F/G 17/2.1
PERFORMANCE OF A PHASE COMPARISON SPREAD SPECTRUM RECEIVER.(U)
DEC 78 J G PENNETT

UNCLASSIFIED AFIT/GE/EE/78-36 NL

1 OF 1
AD
A064369

END
DATE
FILMED
4 -79
DDC

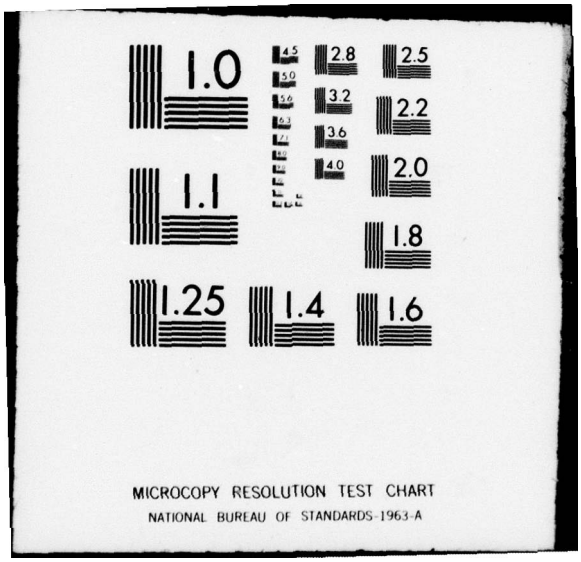
1.0
1.1
1.25
1.4
1.6
1.8
2.0
2.2
2.5
2.8
3.2
3.6
4.0
4.5
5.0
MICROCOPY RESOLUTION TEST CHART
NATIONAL BUREAU OF STANDARDS-1963-A

AFIT/GE/EE/78-36

(1)

LEVEL II

AD A064369

See back page for 1473

DDC FILE COPY

PERFORMANCE OF A PHASE COMPARISON SPREAD SPECTRUM RECEIVER THESIS

AFIT/GE/EE/78-36

JOHN G. PENNETT
Capt USAF

Approved for public release; distribution unlimited.

AFIT/GE/EE/78-36

PERFORMANCE OF A PHASE COMPARISON SPREAD SPECTRUM RECEIVER

THESIS

Presented to the Faculty of the School of Engineering
of the Air Force Institute of Technology
Air Training Command
in Partial Fulfillment of the
Requirements for the Degree of
Master of Science in Electrical Engineering

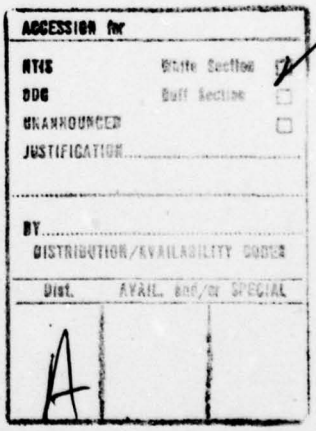

by

John Gary Pennett, B.S.E.E.
Capt USAF
Graduate Electrical Engineering

December 1978

Approved for public release; distribution unlimited.

Preface

> "This is Blue Squadron Leader. They're jamming our communications over the target -- switch to SS mode."

This could have been a line from Star Wars or a military pilot in our next armed conflict. Times have long since past when wars were won by the side with the bigger stick. In this age of electronic wizardry, the side that pushes the state-of-the-art has the upper hand. This paper investigates the use of charge-coupled devices (CCDs) in spread spectrum receivers which even up the size of the sticks in the jamming environment. Since all communications texts use different notation, some familiar benchmark results are presented to provide a point of calibration.

Working on this thesis with the assistance of Captain Stan Robinson as advisor was a refreshing experience. It would not be fair to thank any one person for the behind the scenes work in putting this thesis together; so thanks are due to Mrs. Lana Apana for making these words and equations come to life. I am endeared to Susan, Michael and Cory for their total support during my entire AFIT program.

Contents

List of Figures

List of Tables

Abstract

A phase comparison receiver is implemented at baseband with charge-coupled device (CCD) correlators as matched filters. The received signal is a pseudo-noise (PN) phase coded spread spectrum waveform. The effects of doppler-induced frequency instabilities on the probability of error performance is examined with the differential phase modeled as a Gaussian process. Numerical results are presented and when the variance is greater than 0.1 radians^2 the performance degrades rapidly. An analytic approximation is given for probability of error for specific cases and is useful for small values of variance and low signal-to-noise ratios. In the limit when the variance approaches zero, the receiver performance expression is equivalent to the differentially coherent phase shift keyed (DPSK) receiver. If the reference is perfect in addition to the zero phase variance the performance is the same as a phase coherent receiver with a perfect reference.

I. Introduction

Electronic warfare has come a long way since the days when the bad guys would cut the telegraph lines to the unfortunate town. Electronic warfare cannot be ignored; it is a significant present-day reality which must be countered with state-of-the-art technology. The simplest method of denying our pilots the use of their radio communications is to overpower (jam) their transmissions. One method of increasing the survivability of radio communications in the jamming environment is the spread spectrum modulation technique. Spread spectrum (SS) systems were built as early as the late 1940s (Dixon, 1976:6-7). The hardware complexity of these early receivers filled entire rooms with radio equipment limiting the practicality of their use in many applications. Device technology has advanced since then to the point where spread spectrum transceivers can be contained in handheld units (Dixon, 1976:10).

One particular new device that will be useful in future receiver design is the charge-coupled device (CCD). The CCD was invented in 1970 (Melen, 1977:1), but the need for such a device was overdue and commercially available models are now in production. Unlike a number of spread spectrum correlation techniques, the CCD operates in the baseband frequency range of 1-10 MHz rather than at RF or IF frequencies. Baseband processing of coherent signals requires that either the RF carrier be phase-locked to the local oscillator or that both quadratures of of the RF signal be processed and recombined at baseband to

eliminate the phase differences between the local oscillator and received signal. In this paper, the phase compensation will be accomplished using the latter method where both quadratures will be used for baseband processing.

The phase offset between the received signal and receiver local oscillator is assumed to be a result of air-to-air or air-to-ground communication and is, therefore, referred to as doppler shift. However, the model for phase instability can be extended to analyze the effects of phase shift due to oscillator drift, atmosphere and other common disturbances. In this paper, spread spectrum receivers using CCD code correlators are developed and analyzed for binary signalling probability of error performance.

Background

There are four basic techniques for spread spectrum modulation discussed in the literature (Dixon, 1976): direct modulated sequences, frequency hopping, pulsed-FM or chirp, and time hopping. The receivers discussed in this paper use exclusively the direct sequence format. One method of generating a direct sequence spectrum from binary data is to multiply a data bit by a pseudo-random code. The code bits or chips, as they are more commonly known, are of much shorter duration than the data bits. The resultant signal is used to modulate an RF carrier. Since the chip time dominates or masks the data, the side lobes of the frequency spectrum are spaced farther apart. Additionally, the power in the signal remains the same as the unspread signal; hence, the power density is reduced. Figure 1 shows the frequency spectrum of a

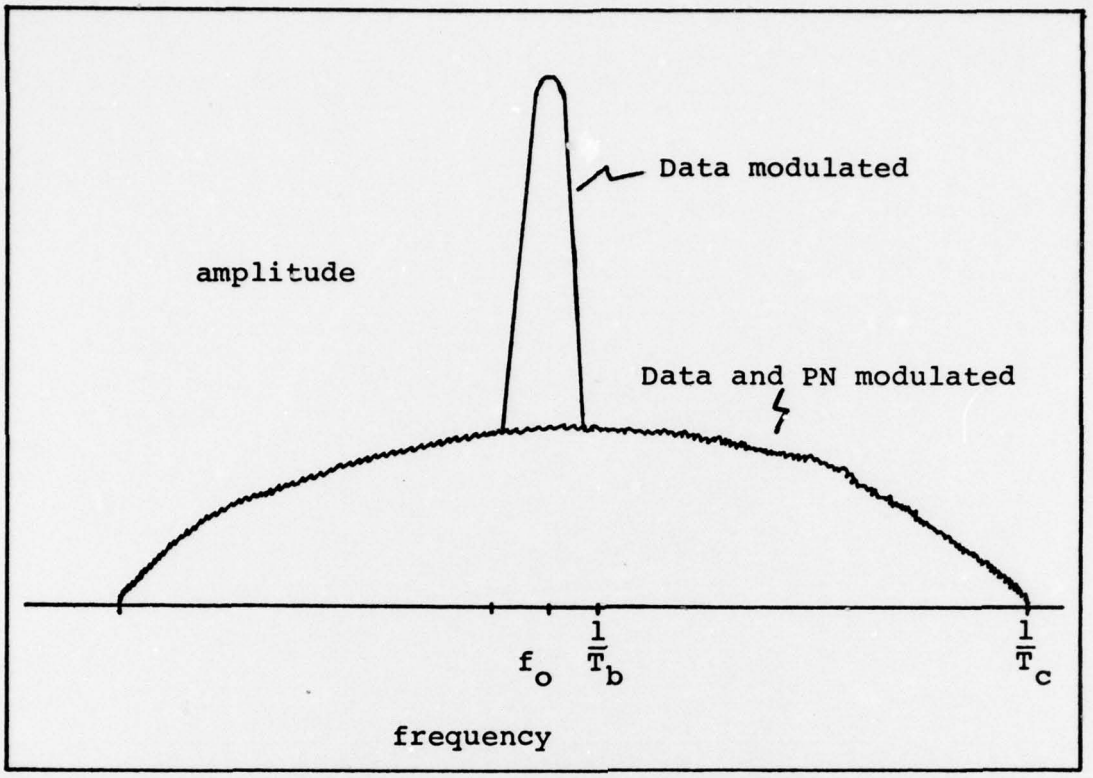

Figure 1. Data Modulated Carrier and PN Modulated Carrier

direct sequence modulated carrier versus the data modulated carrier.

The price for increased resistance to jamming is an increase in the complexity of processing requirements. The CCD has many desirable features necessary in the processing of spread spectrum signals. The CCD provides a flexible interface between continuous analog signals and sampled data processing. Additionally, it is easily adapted to microprocessor control which adds flexibility in adaptive processing and decoding.

Objectives

The scope of this paper includes design and (binary) probability of error performance of a spread spectrum receiver using CCD code correlators. The binary probability error performance is considered for different energy per bit-to-noise spectral density ratios and doppler rates. The receiver noise is white Gaussian noise (WGN) and the doppler is due to the relative motion between receiver and transmitter.

The receivers analyzed do all processing, including doppler phase tracking, at baseband. The local oscillator/mixer will always be tuned to the transmit frequency. However, it is not a voltage controlled oscillator nor is it phase-locked via a phase-lock loop (PLL).

Approach

This report is organized into three main sections with a chapter to cover each topic. Chapter II explains the CCD correlator and the baseband output signal that is common to all receivers. A set of benchmark receivers are discussed in Chapter III as a basis of comparison for error performance. The spread spectrum receivers are also developed and analyzed for error performance in Chapter III. Conclusions and recommendations are included in Chapter IV. The appendices contain some of the more involved and detailed derivations necessary for analysis. When the results of a calculation or derivation are included in the appendix, it is mentioned in the corresponding section of the text.

Chapter II. Received Signal and CCD Model

The received signal and the CCD code correlators are discussed in this chapter. Each signal quadrature is processed through the code correlators, with the resultant sampled data quadrature values processed by the baseband receiver.

Received Signal Model

The received waveform consists of a binary phase shift keyed (BPSK) signal component and a white Gaussian noise (WGN) component due to receiver noise and broadband jammers. The received waveform is given by Eq (1).

$$r(t) = s(t) + n(t) \qquad o \leq t \leq T_b \qquad (1)$$

where

$s(t)$ is the signal

$n(t)$ is the noise

The noise is WGN with a double sided spectral density of $1/2\ N_0$ watts/Hz. In addition to natural sources of noise, additional noise power from a jammer, assuming the jammer is using broadband noise is included in the $1/2\ N_0$ term. The signal portion of the received signal is given by:

$$s(t) = \sqrt{2}Ad(t)c(t)\cos(2\pi f_0 t + \theta(t)) \qquad o \leq t \leq T_b \qquad (2)$$

where

A is the amplitude of the received signal

$d(t)$ is the data waveform, $d_1(t) = -d_2(t) = 1$

$c(t)$ is the PN chip waveform, $|c(t)| = 1$

θ is the random phase difference between the received signal and local oscillator due to transmit and receive oscillator phase difference, doppler, and delay

Each term is assumed to have the following properties throughout the analysis. The amplitude term A is a constant. The data waveform $d(t)$ is equiprobable and has a value $d_1(t) = -d_2(t)$ and $|d(t)| = 1$ for a bit time T_b seconds. Similarly, the chip waveform is $c(t)$ with $|c(t)| = 1$ for T_b seconds and varies at a chip rate R_c which is much faster than the bit rate $R_b = 1/T_b$. The carrier frequency f_0 is constant and known to the receiver. The description of the phase $\theta(t)$ is covered in the next section.

Statistical Model for Phase Offset

The change in phase $\theta(t)$ is assumed to be due to the relative motion between the transmitter and receiver. For example, if the receiver and transmitter are aboard two different aircraft, the relative velocity between the two aircraft depends on their speed and direction. If the aircraft are traveling alongside each other, their relative velocity may be zero, in which case the instantaneous doppler frequency is $d\theta(t)/dt = 0$ Hz. If the aircraft are traveling away from or toward each other along the same velocity vector, the instantaneous frequency is given by:

$$\frac{d\theta(t)}{dt} = \left| \frac{\bar{V}_1 - \bar{V}_2}{c} \right| \cdot f_0 \text{ Hz} \equiv f_d \qquad (3)$$

where

$\bar{V}_1$ and $\bar{V}_2$ are the velocity vectors of aircraft 1 and 2 respectively

c is the speed of light

f_0 is the carrier frequency

A statistical model for the phase process is assumed moderately wide sense stationary over several bit times such that:

$$E[\theta(t)] = \theta_0 \text{ radians} \qquad (4)$$

where

$E[x]$ is the expected value or ensemble average of the waveform $x(t)$ (Papoulis, 1965:138-151).

The generic receiver is a phase comparison receiver where the previously received phase is used as the reference of the present phase. A differential phase process generated by sampling $\theta(t)$ at the bit times is of primary interest rather than the density of $\theta(t)$. The differential phase process $\Delta\theta(t)$ will be defined in terms of the known parameters of f_d and

the correlation properties of $\theta(t)$. The fluctuation in $\theta(t)$ is assumed to be due only to doppler as a result of relative vehicle velocity. A new zero mean process $\theta_d(t)$ thus is given by:

$$\theta_d(t) = \theta(t) - \theta_0 \tag{5}$$

The variance of the first derivative will be defined as the maximum mean squared doppler frequency (Papoulis, 1965: 339):

$$E\left[\frac{d\theta^2 d}{dt^2}\right] = E\left[\frac{d\theta^2}{d_{t^2}}\right] \tag{6}$$

$$E\left[\frac{d\theta_d}{dt} \cdot \frac{d\theta_d}{dt'}\right] = \frac{-\partial^2 R_{\theta d}(T)}{\partial T^2} \tag{7}$$

where

$$\left.\frac{-\partial^2 R_{\theta d}(T)}{\partial T^2}\right|_{T=0} \equiv f'^2_d \tag{8}$$

$$T \equiv |t-t|$$

$$f'_d \equiv \left|\frac{\bar{V}_1 - \bar{V}_2}{c}\right| \max \cdot f_0$$

$R_x(T)$ is the correlation of the function of the process x

The correlation function of $\theta_d(t)$ is assumed to be a Gaussian shaped function as the second derivative exists everywhere and is given by:

$$R_{\theta_d}(T) = \sigma_{\theta_d}^2 \exp(-T^2/\eta^2) \tag{9}$$

The value of $\sigma_{\theta_d}^2$ can be defined in terms of the second partial derivative of $R_{\theta d}(T)$. On computing the second partial as in Eq (7) and solving for $\sigma_{\theta_d}^2$ the result is:

$$\sigma_{\theta d}^2 = \frac{f_d'^2 \eta^2}{2} \tag{10}$$

The correlation time is given by (Lindsey, 1973:313):

$$T_c \sigma_{\theta_d}^2 \equiv \int_0^\infty \left| R_{\theta d}(T) \right| d_T \tag{11}$$

Using Eq (9) and solving for T_c gives:

$$T_c = \frac{\eta}{2} \sqrt{\pi} \tag{12}$$

The CCD code correlators require the phase to be relatively constant over a symbol interval T_b a point that will become apparent in the next section on the CCD code correlators. Typically, the phase can be considered constant over a symbol interval if (Lindsey, 1973:314):

$$T_c \geq 4 T_b \tag{13}$$

In terms of η :

$$0 \leq T_b \leq \frac{\eta}{8}\sqrt{\pi} = \frac{T_c}{4} \tag{14}$$

The value of T_b is limited by T_c which is in turn a function of the dynamics of the aircraft in relation to each other during a typical mission. Useful values of T_c are not presently available and are left unspecified as is f'd. The results are then applicable in the most general case. The differential process is given by:

$$\Delta\theta(t) = \theta(t) - \theta(t - T_b) \tag{15}$$

The statistics of $\Delta\theta$ are

$$E[\Delta\theta] = 0 \tag{16}$$

and (Papoulis, 1965:336-381):

$$R_{\Delta\theta}^{(T)} = 2R_{\theta d}(T) - R_{\theta d}(|T_b - T|) - R_{\theta d}(T_b + T) \tag{17}$$

Since $\Delta\theta$ is a zero mean, the variance is given by:

$$\sigma_{\Delta\theta}^2 = R_{\Delta\theta}(o) = 2\sigma_{\theta d}^2 (1 - \exp(-T_b^2/\eta^2)) \tag{18}$$

Using Eq (14), the admissible range of the variance of $\Delta\theta$ is thus given by:

$$0 \leq \sigma_{\Delta\theta}^2 \leq .1\ \sigma_{\theta d}^2 = \frac{f'^2_d\ T_c^2}{5\pi} \qquad (19)$$

The range of $\sigma_{\Delta\theta}^2$ is now defined in terms of measurable parameters T_c and f_d. Information on a useful density of $\Delta\theta$ was not available at this writing; however, it is reasonable to assume that the $\Delta\theta$ is distributed as a zero mean Gaussian random variable with $\sigma_{\Delta\theta}^2$ given by Eq (18). A useful density which exhibits properties similar to a Gaussian density but is limited to $\pm\ \pi$ is given by:

$$f(\Delta\theta) = \frac{\exp\ (\alpha\ \cos\ \Delta\theta)}{2\pi\ I_0\ (\alpha)} \qquad (20)$$

where

I_0 is modified Bessel function of the first kind of order zero

α is approximately $\frac{1}{\sigma_{\Delta\theta}^2}$ for $\alpha > 4$ or $\sigma_{\Delta\theta}^2 < .25$ (Viterbi, 1966:92-95)

The density in Eq (20) will be used for the statistical model of $\Delta\theta$ as in addition to its Gauss-like characteristics, it has well defined higher order moment properties in $\cos\theta$ and $\sin\theta$ which will be of value when investigating the quadrature representations of the received signal (Lindsey, 1973:36).

CCD Model

CCDs have only recently become available to designers in commercial quantities in both analog and digital configurations

(Melen, 1977). A wide variety of CCD models exist for analog signal processing, consequently the mathematical model derived for analysis is based on a specific correlator; the General Electric CR series of CCD correlators (Buss, 1973).

A CCD configured as an analog correlator consists of a number of charge storage bins or stages. The amount of charge in each bin is proportional to the input signal level and an integration time during which the bin is filled with a charge. A typical CR correlator consists of 32 stages and several CRs can be cascaded to form correlators of multiples of 32 stages.

The CR correlators operate on a moving reference rather than a moving charge principle. The moving reference CCD configuration reduces the number of singal packet shifts which improves efficiency of the device (Buss, 1973:83-90). A block diagram of the correlator is shown in Figure 2.

In order to simplify the analysis, the effects of attentuation and noise added by the CCD will not be included in the derivation of the output statistics of the code correlators. The inclusion of the effects of attentuation and noise in the CCD would not drastically change any results as the loss through a CCD of 32 stages is on the order of fractions of a dB and the CCD internal noise is considerably less than the receiver input noise (Buss, 1973:90).

The correlators are connected to form the desired receiver as shown in Figure 3. The output of the multipliers with s(t) as the input ignoring double frequency terms (as the frequency

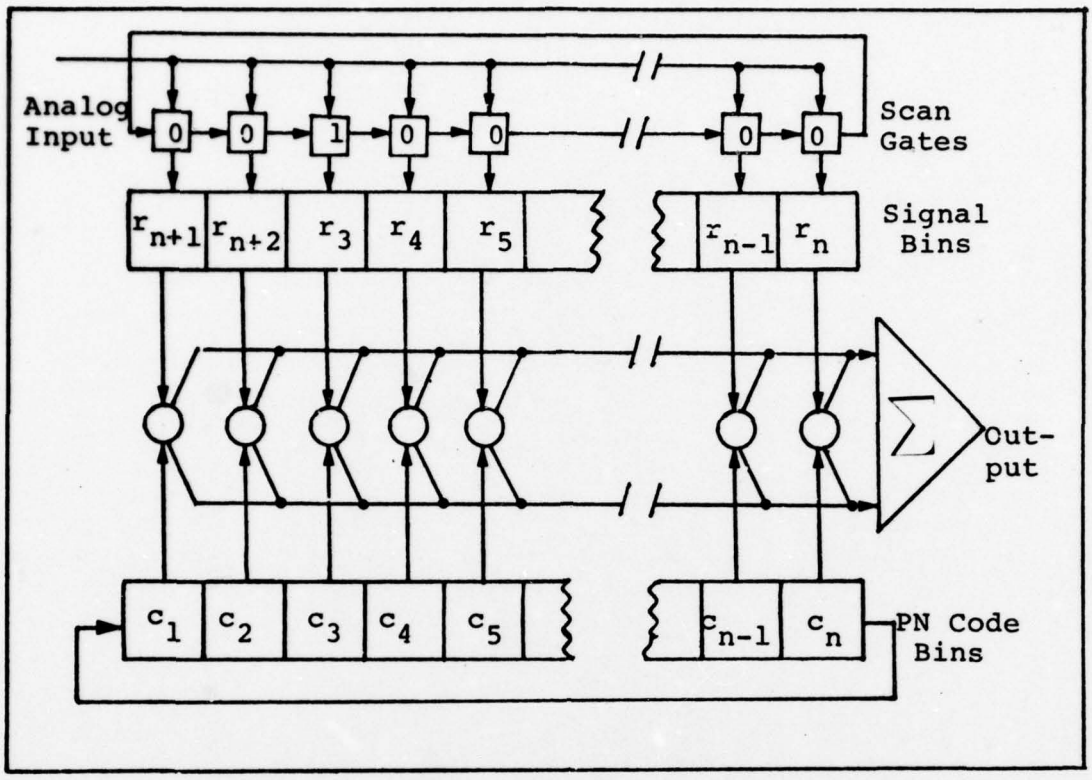

Figure 2. Moving Reference CCD Code Correlator.

characteristics of most multipliers do not cover such a wide frequency range) is:

$$s(t)(\sqrt{2}\cos 2\pi f_0 t) = S_I(t) \tag{21}$$

then:

$$S_I(t) = Ad(t)c(t)\cos\theta(t) \tag{22}$$

similarly

$$S_Q(t) = Ad(t)c(t)\sin\theta(t) \tag{23}$$

Fig 2

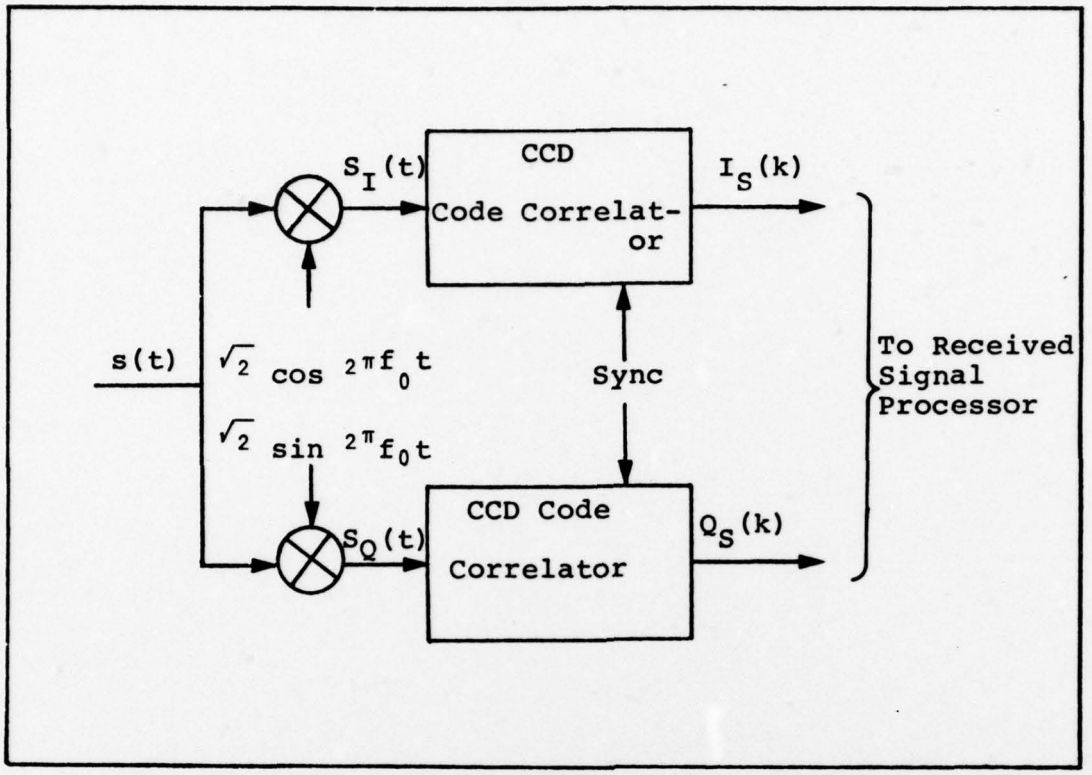

Figure 3. Received Signal Multipliers and Code Correlators.

The signal output of the correlators is given by:

$$I_s(k) = \sum_{i=1}^{N} c(i) \int_{(i-1)T_c + kT_b}^{iT_c + kT_b} S_I(t)\,dt \qquad (24)$$

The code chips c(i) are ± 1 and assumed to be properly aligned with the received bit. The result of the integration and summation is:

$$I_s(kT_b) \equiv I_s(k) = ANT_c d(K) \overline{\cos \theta(k)} \qquad (25)$$

similarly

$$Q_s(k) = ANT_c d(k) \overline{\sin \theta(k)} \tag{26}$$

where

N is the number of correlation stages (also the number of chips in code bit)

(k) is the notation for (kT_b) and the T_b is omitted to simplify notation

Because of the restrictions imposed on the phase process $\theta(t)$, the phase is constant over a symbol interval of T_b seconds and $\overline{\cos \theta(k)}$ is given by (Lindsey, 1973:312):

$$\overline{\cos \theta(k)} = \frac{1}{T_b} \int_{kT_b}^{(k+1)T_b} \cos \theta(t)\, dt \tag{27}$$

with a similar expression for $\overline{\sin \theta(k)}$.

The statistics of the output noise $N_I(k)$ are:

$$E[N_I(k)] = E\left[\sum_{i=1}^{N} \sqrt{2} \int_{0}^{kT_b + T_c} n(t) \cos 2\pi f_0 + dt \right] \tag{28}$$

$$= 0$$

where

$$\frac{1}{T_c} << f_0$$

The variance is given by:

$$E[N_I^2(k)] = 2E\left[\sum_{i=1}^{N}\sum_{j=1}^{N} c(i)c(j)\int_{(j-1)T_c}^{jT_c}\int_{(i-1)T_c}^{iT_c} n(\alpha)n(\beta)\cos(2\pi f_0\alpha)\cdot\cos(2\pi f_0\beta)\,d\alpha d\beta\right]$$

$$= 2E\left[\sum_{i=1}^{N}\iint_{(i-1)T_c}^{iT_c} n(\beta)n(\alpha)\cos(2\pi f_0\alpha)\cos(2\pi f_0\beta)\,d\alpha d\beta + \sum_{i\neq j}^{N}\sum^{N}\int_{(j-1)T_c}^{jT_c}\int_{(i-1)T_c}^{iT_c} n(\alpha)n(\beta)\cos(2\pi f_0\alpha)\cos(2\pi f_0\beta)\,d\alpha d\beta\right] \quad (29)$$

The cross product terms $(i \neq j)$ are zero since the noise samples are independent. On computing the expected value of the summation in Eq (29) when $i = j$ the variance is:

$$E[N_I(k)^2] = 1/2N_oT_cN \quad (30)$$

The variance for the other noise quadrature is computed in the similar manner and the result is:

$$E[N_Q(k)^2] = 1/2N_oT_cN \quad (31)$$

The signal to noise on each quadrature is defined by (Ziemer, 1976:303-315):

$$SNR_c = \frac{E[I(k)^2]}{E[N_I(k)^2]} \tag{32}$$

$$SNR_s = \frac{E[Q(k)^2]}{E[N_Q(k)^2]} \tag{33}$$

The signal to noise input to the received signal processor is defined as the SNR_c with $\theta(t) = 0$. The output of each quadrature is given by:

$$I(k) = I_s(k) + N_I(k) \tag{34}$$

$$Q(k) = Q_s(k) + N_Q(k) \tag{35}$$

Note that the expected value of I(k) and Q(k) in Eqs (32) and (33) is the signal portion of Eqs (34) and (35), respectively.

Using the value of $I_s(k)$ from Eq (25) with $\theta(k) = 0$ and noting that $d(k)^2 = 1$ the signal to noise is:

$$SNR = \frac{A^2N^2T_c^2}{N_oN\,T_c} \tag{36}$$

Recalling that $NT_c = T_b$, we will see later that the performance will be expressed in terms of energy-per-bit to noise spectral density given by:

$$R = \frac{A^2NT_b}{N_o} \tag{37}$$

The model for phase and the expression for energy per bit-to-noise is used throughout the remainder of this paper. The output of the correlators in Eqs (34) and (35) is the input signal used by the receivers throughout the remainder of this paper.

Chapter III. Receiver Design and Performance

The spread spectrum receivers are designed and analyzed in this chapter. Prior to embarking on the development and performance of specific receivers, the results for some standard benchmark receivers are presented to provide a point of reference. The approach to the design of the spread spectrum receivers will begin with the development of a generic receiver with generalized performance results. The generic model is followed by some special cases.

Benchmark Receivers

The results for two benchmark receivers are presented in this section. The first is a coherent receiver with a perfect reference, and the second is a differentially phase shift keyed (DPSK) receiver with the signal phase constant during a symbol interval of $2T_b$ seconds.

Coherent Benchmark Receiver

The classical phase coherent receiver consists of a local oscillator tuned to the received signal carrier with no phase offset. A block diagram of the receiver is shown in Figure 4, where $r(t)$ is given by Eq (1). As before, the clock is synchronized to integrate each chip for a period of T_c seconds and the data bit is correlated and sampled every T_b seconds. The output $I(k)$ is given by:

$$I(k) = Ad(k)NT_c + N_I(k) \tag{38}$$

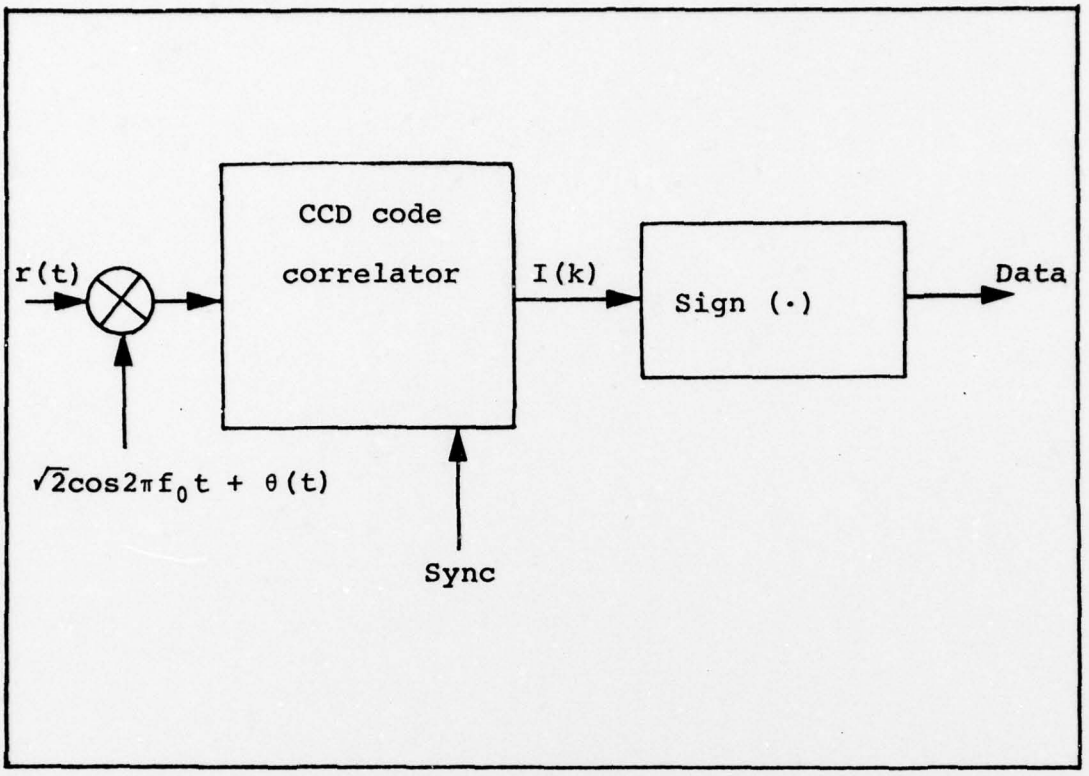

Figure 4. Coherent Benchmark Receiver.

Using the results from Chapter II and from Figure 4 $\theta(k+i) = 0$ the performance is given by (Van Trees, 1968: 98-102):

$$P_e = 1/2 \text{ erfc } (\sqrt{R}) \tag{39}$$

where

R is defined in Eq (37) as only the SNR term is present and

$$\text{erfc}(y) \equiv \int_y^\infty \frac{2}{\sqrt{\pi}} \exp [x^2] \, dx$$

The next logical step is to graph P_e versus R, but this step will be postponed until both benchmark results are presented.

DPSK Benchmark Receiver

The DPSK receiver uses the previous bit as a reference for the next bit. The assumption is made that for this receiver s(t) is differentially encoded at the transmitter. Since the previous data bit is used for a reference, a locally generated synchronized carrier is not necessary, thus coherent carrier detection synchronization circuits such as phase-locked loops are not necessary. The diagram for the baseband DPSK receiver is shown in Figure 5.

The performance for the DPSK receiver is derived in many texts (Downing, 1964:184-187); (Lindsey, 1973:245-252); and (Spilker, 1977:336). In all of these texts, the assumption is made that the phase is constant, but unknown over $2T_b$ seconds and the only corruption of phase is due to Gaussian noise. In terms of the model for the doppler phase given in Chapter II, the variance $\sigma_{\Delta\theta}^2 = 0$. Various methods are given for deriving the performance and the result in all cases is:

$$P_e = 1/2 \exp(-R) \qquad (40)$$

The P_e versus R is plotted for both benchmark receivers in Figure 6.

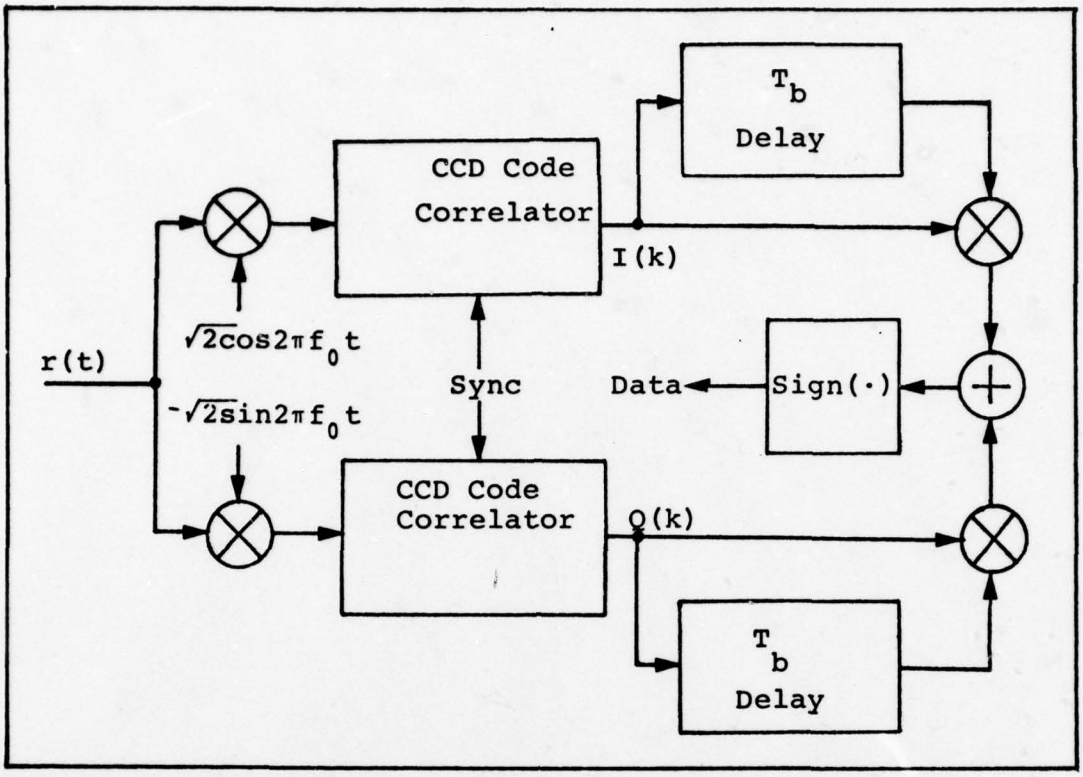

Figure 5. DPSK Benchmark Receiver.

Generic Spread Spectrum Receiver

A generalized diagram of the spread spectrum receivers analyzed in this section is given in Figure 7. An expression for performance will be presented in general and special cases with typical values graphed to compare performance.

The decision variable W(k) in Figure 7 can be defined as consisting of two possible signals. The signals are a reference vector composed of $\hat{I}(k)$ and $\hat{Q}(k)$ and a data measurement vector I(k) and Q(k) in vector notation rewritten as:

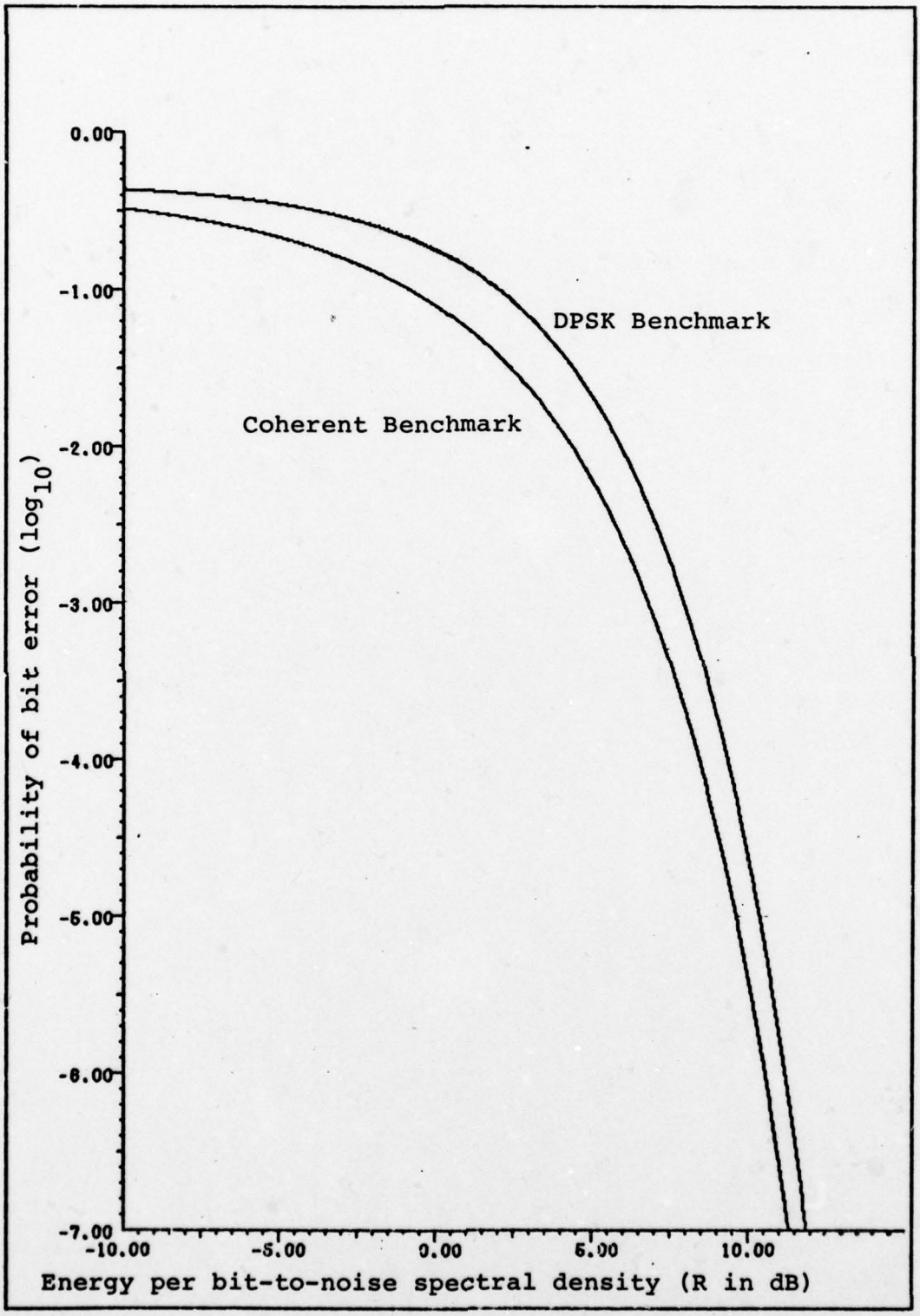

Figure 6. Probability of Error Performance for Benchmark Receivers.

$$\bar{U}(k) = \begin{bmatrix} \hat{I}(k) \\ \hat{Q}(k) \end{bmatrix} \tag{41}$$

$$\bar{S}_0(k) = \begin{bmatrix} I(k) \\ Q(k) \end{bmatrix} \tag{42}$$

The optimum decision is given by (Wozencraft, 1968:214-217):

$$\bar{U}(k)^T \bar{S}_0(k) \underset{0}{\overset{1}{\gtrless}} \tag{43}$$

where

$x \underset{b}{\overset{a}{\gtrless}} y$ is the double inequality when $x>y$ a is chosen and when $x<y$ b is chosen

$x^{-T}\bar{y}$ is the inner produce of vectors $\bar{x}$ and $\bar{y}$

The characteristics of $\bar{U}$ depend on the configuration of the particular receiver. In each of the special cases of receivers developed, the form of the vector $\bar{U}$ will change and $\bar{S}_0$ will be defined in Eq (42). The characteristics of $\hat{I}$ and $\hat{Q}$ will be altered to develop various forms of the vector $\bar{U}$.

The error performance of the generic receiver is given by (Stein, 1964:43-51):

$$P_{e|\Delta\theta} = Q(\sqrt{a}, \sqrt{b} - \frac{\sigma^2 s}{\sigma^2 s + \sigma^2 u} \exp\left[-\frac{a+b}{2}\right] I_0(\sqrt{ab}) \tag{44}$$

with an alternate form given by:

$$P_{e1\Delta\theta} = 1/2\ [1-Q(\sqrt{b},\ \sqrt{a}) + Q(\sqrt{a},\ \sqrt{b})]$$

$$- \frac{\sigma^2_s - \sigma^2_u}{2(\sigma^2_s + \sigma^2_u)} \exp\left[-\frac{a+b}{2}\right] I_0\ (\sqrt{ab}) \qquad (45)$$

where

Q is the Marcum Q function and is discussed in Appendix A.

I_0 is the modified Bessel function of the first kind of order zero and is also discussed in Appendix A.

σ^2_s is the variance of the data vector terms I(k) and Q(k)

σ^2_u is the variance of the reference vector terms $\hat{I}(k)$ and $\hat{Q}(k)$

The terms a and b are given in general as (Stein, 1964:50):

$$a = \left\{ \frac{E[I(k)]^2 + E[Q(k)]^2}{\sigma^2_s} + \frac{E[\hat{I}(k)]^2 + E[\hat{Q}(k)]^2}{\sigma^2_u} - \frac{2}{\sigma_s\ \sigma_u}\left[E[I(k)]\ E[\hat{I}(k)] + E[Q(k)]\ E[\hat{Q}(k)]\right]\right\} \qquad (46)$$

$$b = \left\{ \frac{E[I(k)]^2 + E[Q(k)]^2}{\sigma_s{}^2} + \frac{E[\hat{I}(k)]^2 + E[\hat{Q}(k)]^2}{\sigma_u{}^2} + \frac{2}{\sigma_s\sigma_u}\left[E[I(k)]\ E[\hat{I}(k)] + E[Q(k)]\ E[\hat{Q}(k)]\right]\right\} \qquad (47)$$

where

$E[\cdot]$ is the average over the Gaussian noise statistics conditioned on the doppler phase $(\Delta\theta)$ known

The terms a and b as defined in Eqs (46) and (47) assume the doppler phase $\Delta\theta$ in Eqs (25) and (26) to be some constant value; hence, the phase is not averaged in the expected value in Eqs (46) and (47). The terms a and b can be written in terms of R as given in Eq (37) for $\overline{S}_o$ and βR for the energy per bit-to-noise spectral density of $\overline{U}$. The terms a and b with $\Delta\theta$ known are rewritten:

$$a = \frac{R}{2}\left[(1 + \beta) - 2\sqrt{\beta}\cos\Delta\theta\right] \tag{48}$$

$$b = \frac{R}{2}\left(1 + \beta) + 2\sqrt{\beta}\cos\Delta\theta\right] \tag{49}$$

where

$\Delta\theta$ is the angle between the signal components of $\overline{S}_o$ and $\overline{U}$

β is the ratio of energy per bit-to-noise spectral density ratio of the $\overline{U}$ reference and $\overline{S}_o$ data vector.

The term β is considered to be greater than or equal to one for all cases considered. It is tempting at this point in the analysis to average $\cos\Delta\theta$ over the statistics for $\Delta\theta$ in Eq (20); however, the Q function is not a linear

operation, and the expected value operation on $\Delta\theta$ cannot be interchanged. The required operation for average probability of error performance is given by:

$$P_e = \int_{-\pi}^{\pi} P_{e|\Delta\theta} \, f(\Delta\theta) \, d\Delta\theta \tag{50}$$

where

$P_{e|\Delta\theta}$ is the conditional probability of error expression in Eq (44) or (45) with $\Delta\theta$ known

The density $f(\Delta\theta)$ is rewritten from Chapter II Eq (20) for reference:

$$f(\Delta\theta) = \frac{\exp(\alpha\cos\Delta\theta)}{2\pi I_0(\alpha)} \tag{51}$$

The average given on the right side of Eq (50) is not a trivial operation and a closed form solution for the general case possibly does not exist. There are a few limiting cases and special configurations of the generic receiver where approximations for error performance are useful. A realistic operational range of interest is the required energy per bit-to-noise spectral density that has an average probability of error on the order of 10^{-3} or 10^{-5} bits per error.

The terms a and b were written with the parameter β as a ratio between the signal bit and reference bit. It is conceivable that the filter in Figure 7 could smooth the previously received vectors and reduce the variance of the

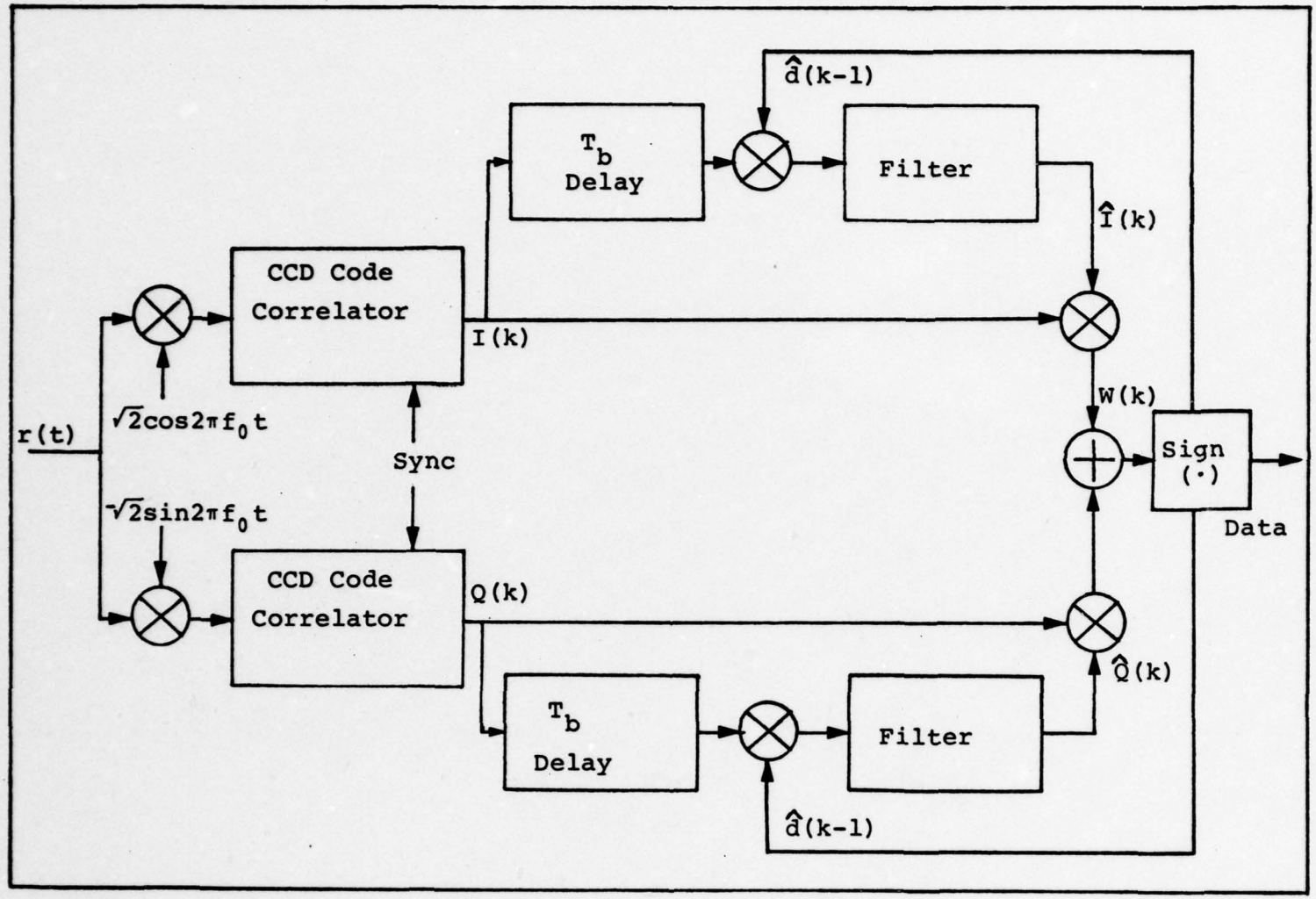

Figure 7. Generic Spread Spectrum Receiver.

$\bar{U}$ vector in which case β would be greater than one. In the case where the filters are absent and there is no data feedback, the typical DPSK receiver results. The term α in Eq (51) is also a variable parameter in system performance controlled by the coherence time of the phase $\Delta\theta(t)$ and the data time T_b. If the filters in Figure 7 could predict the phase of $\bar{S}_o$, then it is conceivable that the variance on the phase could be reduced, thus increasing α $\left(\text{since } \alpha = \frac{1}{\sigma^2_{\Delta\theta}}\right)$. The larger the term α is, the greater the probability that $\Delta\theta$ is close to zero radians. The α and β terms can conceptually be varied independently to determine which parameter has the greatest effect in improving error performance without specifying the filters in Figure 7.

In the next section, various configurations of the generic receiver of Figure 7 will be considered and analyzed for error performance. In the receivers where data feedback is present, the receiver is assumed to be operating with perfect data feedback. Additionally, the variance of the vector components $\bar{S}_o$ and $\bar{U}$ will be assumed equal although β may be greater than one (Stein, 1965:45); with this assumption, only the first half of Eq (45) is necessary for error performance, as $\sigma_s^2 - \sigma_u^2 = 0$.

Generalized Performance Results. A closed form solution to Eq (50) possibly does not exist in which case the only other alternatives are bounds, approximations, or numerical integration. The latter alternative will be presented

first to provide a point of comparison for an approximation which is useful in a limited region.

The Q function routine was not available in the computer library functions; however, a simple recursive method used to generate the Q function tables commonly used in radar-detection theory (Brennan, 1965:312-313) was easily developed using a FORTRAN program and the recursion relation given in Appendix B.

The probability of error was calculated using:

$$P_e = 1/2 \left[1 - \int_{-\pi}^{\pi} Q(\sqrt{b}, \sqrt{a}) f(\Delta\theta) d\Delta\theta + \int_{-\pi}^{\pi} Q(\sqrt{a}, \sqrt{b}) f(\Delta\theta) d\Delta\theta \right] \quad (52)$$

The numerical integration technique requires that the integrand be a function of one variable and the functions in the integral are rewritten:

$$F(x) = Q\left(\sqrt{R/2 \left[(1+\beta) \mp 2\sqrt{\beta} \cos x \right]} \sqrt{R/2 \left[(1+\beta) \mp 2\sqrt{\beta} \cos x \right]} \right) \frac{\exp(\alpha \cos x)}{2\pi I_0(\alpha)} \quad (53)$$

The probability of error in Eq (52) can be rewritten in terms of one variable of integration as

$$P_e = 1/2 \left[1 - \int_{-\pi}^{\pi} F^{+}(x)\, dx + \int_{-\pi}^{\pi} F^{-}(x)\, dx \right] \quad (54)$$

where

$F^+(x)$ is given in Eq (53) with the plus in the first radical and a minus in the second radical in Eq (53).

$F^-(x)$ is the opposite sign under the radical in Eq (53) as $F^+(x)$

The only variable of integration in Eq (54) is x and $F(x)$ can be written as a function subroutine suitable for use in a numerical integration library subroutine. Unfortunately, with even a large computer such as the CDC 6600, each integration takes approximately .3 seconds (with $R_N = 10^{-15}$; see Appendix B) which takes 60 seconds calculating 200 points for plotting; an alternate method is desirable. Graphs of the numerical results are withheld until the approximate result is derived.

From Appendix A, the Q function can be expanded in an infinite series of modified Bessel functions and using a and b as defined in Eqs (48) and (49), the probability of error is rewritten:

$$P_{e/\Delta\theta} = 1/2 \exp\left(\frac{-R(1+\beta)}{2}\right) \cdot \left[I_0(c) + 2 \sum_{n=1}^{\infty} (d)^n I_n(c) \right] \quad (55)$$

where

c is $R/2 \sqrt{(1+\beta)^2 - 4\beta\cos\Delta\theta}$

d is $\sqrt{\dfrac{(1+\beta) - 2\sqrt{\beta}\cos\Delta\theta}{(1+\beta) + 2\sqrt{\beta}\cos\Delta\theta}}$

The form of Eq (55) cannot be integrated directly using $f(\Delta\theta)$ however, the modified Bessel function can also be expanded in a power series and using the first two terms in the power series expansion from Appendix A, the conditional probability of error is rewritten:

$$P_{e|\Delta\theta} = 1/2 \exp\left(\frac{-R(1+\beta)}{2}\right) \cdot \left[2\exp\left(\frac{c}{2}\right) \cdot dc\left(\exp\left(\frac{c}{2}\right)-1\right) - 1 - \frac{c}{2}\right] \quad (56)$$

The expression in Eq (56) can be averaged term-by-term using the circular moment properties of $f(\Delta\theta)$ (Lindsey, 1973: 36), resulting in:

$$P_e \simeq 1/2 \exp\left(\frac{-R(1+\beta)}{2}\right) \cdot \left\{ 2 \exp\left(\frac{R(1+\beta)}{4}\right) \frac{I_0\left(\alpha-\frac{R\sqrt{\beta}}{2}\right)}{I_0(\alpha)} + \frac{R}{2} \left[(1+\beta)\exp\left(\frac{R(1+\beta)}{4}\right) \frac{I_0\left(\alpha-\frac{R}{2}\sqrt{\beta}\right)}{I_0(\alpha)} + 2\sqrt{\beta}\exp\left(\frac{R(1+\beta)}{4}\right) \frac{I_2\left(\alpha-\frac{R\sqrt{\beta}}{2}\right)}{I_0(\alpha)} \right] - (1+\beta) - 2\sqrt{\beta}\,\frac{I_1(\alpha)}{I_0(\alpha)} - 1 - \frac{R^2}{16}\left[(1+\beta)^2 - 2\beta\left(1+\frac{I_2(\alpha)}{I_0(\alpha)}\right)\right] \right\} \quad (57)$$

The resultant expression is rather cumbersome; however, the probability of error can easily be plotted using a computer plotting routine and Eq (57). The range that Eq (57) gives valid results is determined by comparing the numerical results of Eq (54) to the approximate results of Eq (57). The

results for various values of variance of $\Delta\theta$ with $\beta = 1$ are given in Figure 8 thru 12. From the results of Figures 11 and 12, the approximation is within .5 dB of the numerical results for an R necessary for $P_E > 10^{-7}$. The approximation is of little use when $\sigma^2_{\Delta\theta} = .1$ as it is accurate only when $P_E > 10^{-2}$ as can be seen in Figure 8. When $\sigma_{\Delta\theta}{}^2 = .05$, the approximation is useful from R's necessary for $P_E > 10^{-3}$. In Figure 10 the approximation is useful for R's necessary for $P_E > 10^{-4}$. Table I summarizes these results and the approximate values of R for a given P_E with the * indicating those values that the approximation is within 10% of the numerical results. The range for which Eq (57) is useful within 10% of numerical results is $0 \leq \sigma_{\Delta\theta}{}^2 \leq .033$ and R<10dB.

Table I. Required R in dB for a Given Variance and Probability of Error (β=1)

	Numerical Results				
P_E	$\sigma^2_{\Delta\theta}$ = .1	.05	.033	.02	.01
10^{-3}	9.75	8.54	8.29	8.11	7.93
10^{-5}	15	11.78	11.05	10.70	10.48
P_E	Approximate Results				
10^{-3}	8.80	8.36*	8.22*	8.10*	8.02*
10^{-5}	11.35	10.88*	10.72*	10.58*	10.46*
	Benchmark Receivers				
P_E	Coherent ($\beta=\infty$, $\sigma_{\Delta\theta}=0$)		DPSK ($\sigma^2_{\Delta\theta}=0$)		
10^{-3}	6.79		7.93		
10^{-5}	9.58		10.34		

*These values of R are within 10% of the numerical values.

From Table I, the approximation for P_e is very good when $\sigma_{\Delta\theta}^2 < .05$ radians^2 ($\sigma_{\Delta\theta} < 12.8^o$) and $R < 9$dB. The effects of increasing β cannot be demonstrated using Eq (57) as the approximation is useful in an ever-decreasing value of R. The numerical techniques, however, can be used to determine the effect of increasing β. Figures 13 and 14 show the numerical results for two values of $\sigma_{\Delta\theta}^2$ and a few values of β. In the limit, however, as $\beta \to \infty$ the conditional probability of error reduces to (Stein, 1964:44):

$$P_{e|\Delta\theta} = 1/2 \text{ erfc } (\sqrt{R} \cos \Delta\theta) \qquad (58)$$

Averaging Eq (58) results in an infinite series expansion that is evaluated for various values of α in other texts (Lindsey and Simon, 1973:313-316) using $f(\Delta\theta)$ as given by Eq (51). Figure 15 shows the results of integrating Eq (58) over $f(\Delta\theta)$ for the same values of α as given in Figures 8 and 9. A comparison of Figure 13 with Figure 15 for $\sigma_{\Delta\theta}^2 = .1$ and $\beta = 10$ indicates that there is little additional improvement in performance when β is increased from 10 to infinity. This result shows that when $\sigma_{\Delta\theta}^2 > .1$ the variance is the more sensitive performance parameter. The averaging of Eq (58) results in an irreducible error performance; for example, when α is 10 or less ($\sigma_{\Delta\theta}^2 > .1$ rad^2) the receiver will not perform better than 10^{-5} errors per bits for R as high as

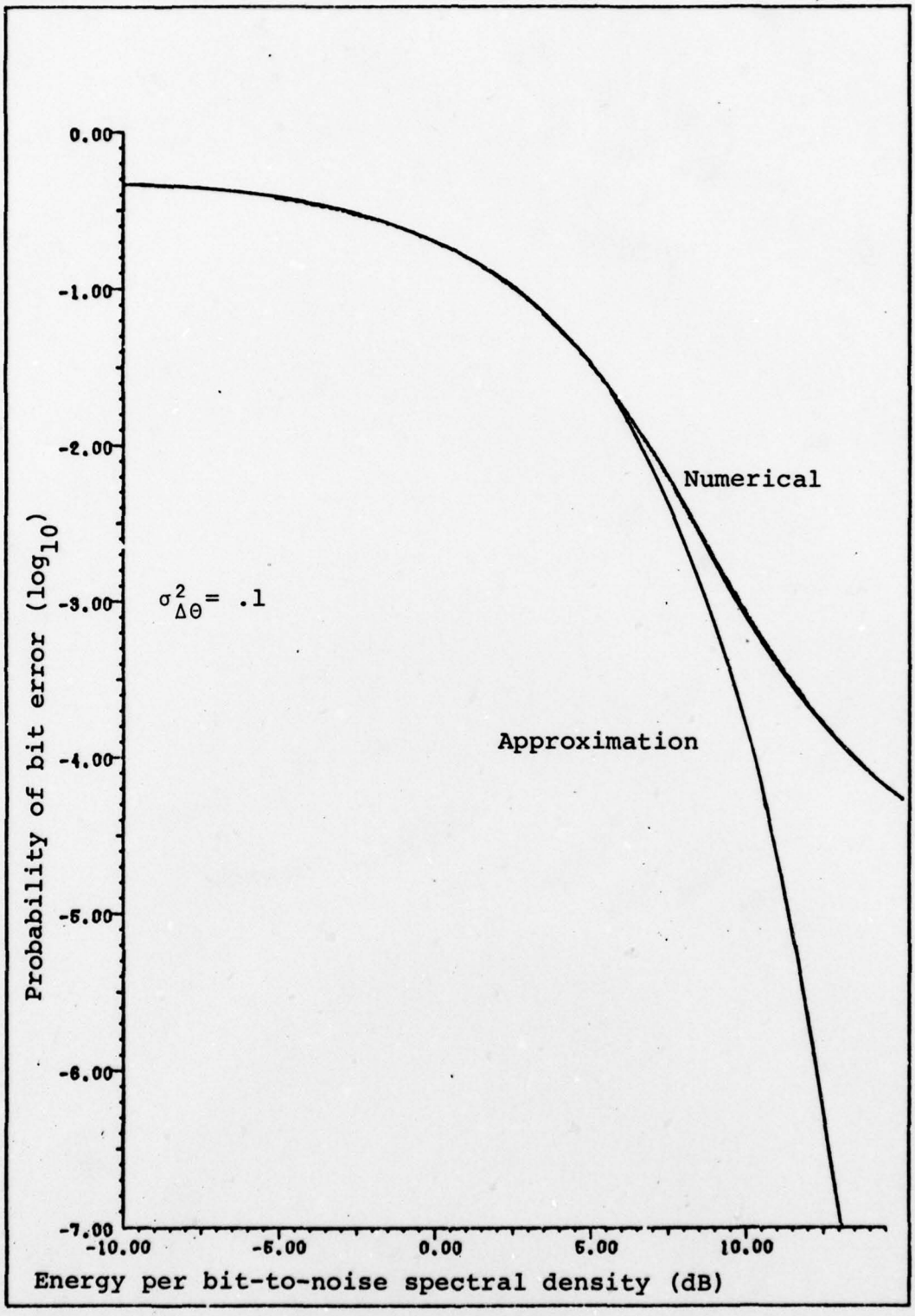

Figure 8. Numerical vs Approximation Probability of Error $\sigma^2_{\Delta\theta}$ = .1 .

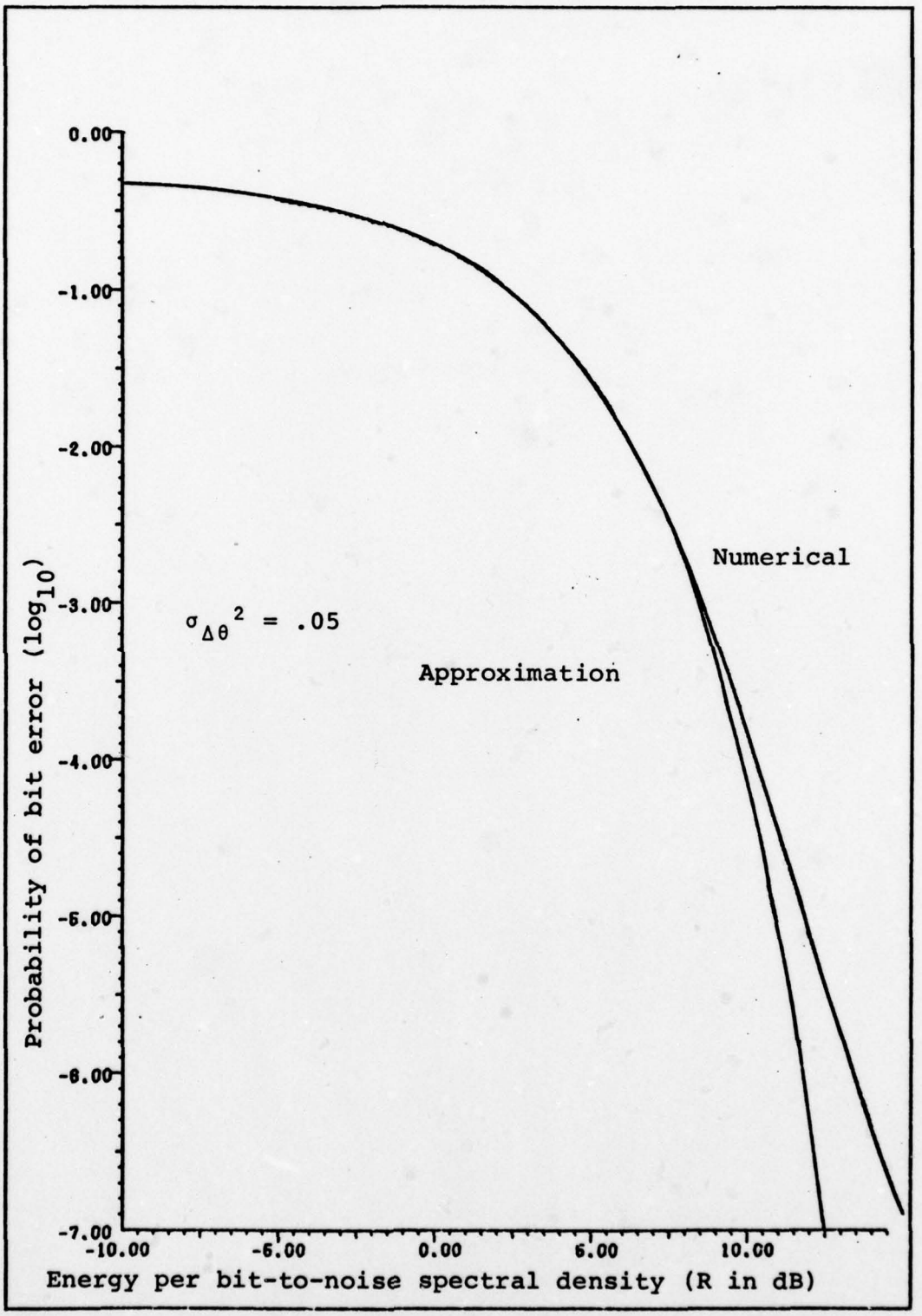

Figure 9. Numerical vs Approximate Probability of Error $\sigma_{\Delta\theta}^2 = .05$.

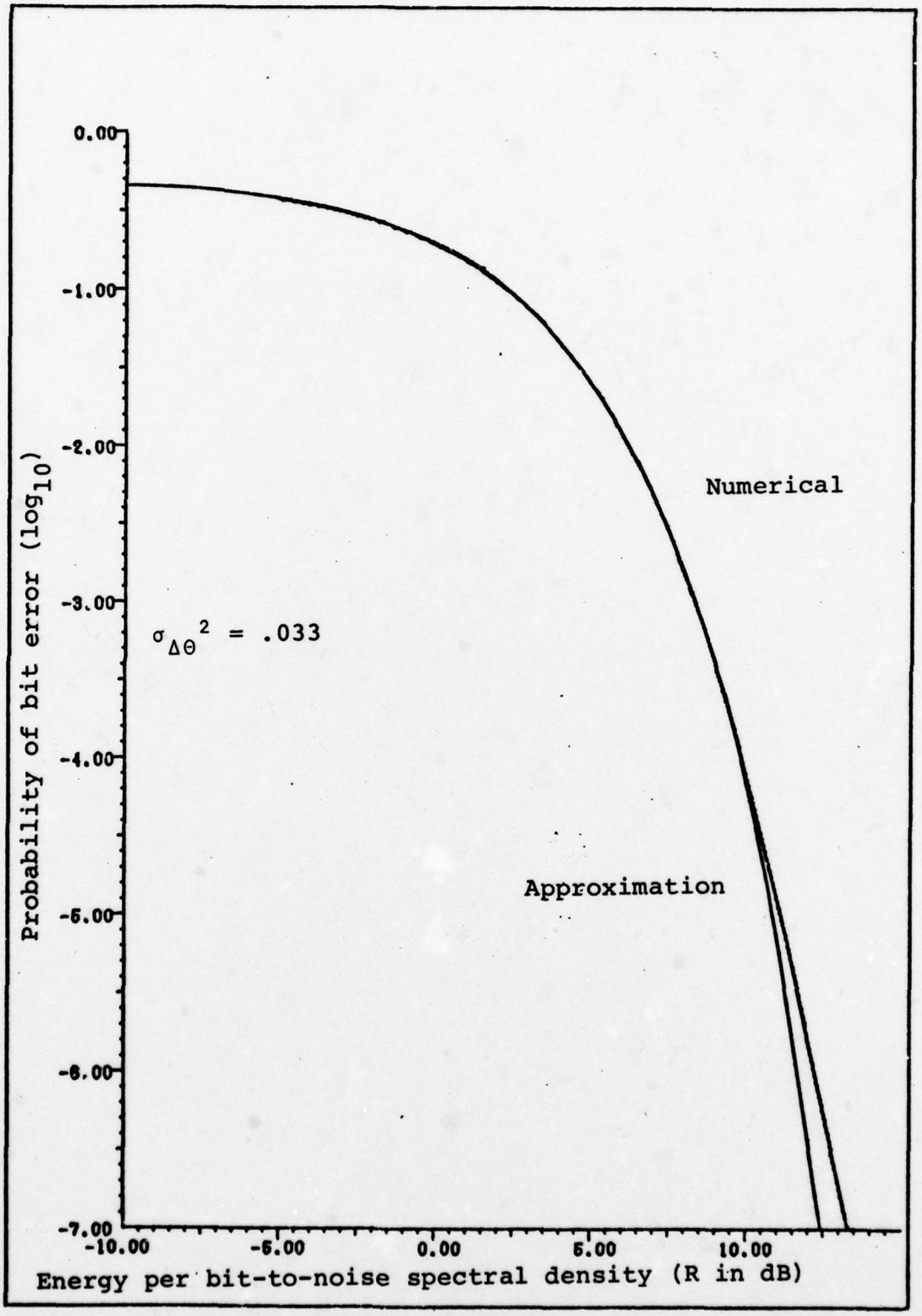

Figure 10. Numerical vs Approximate Probability of Error $\sigma_{\Delta\Theta}^2 = .033$.

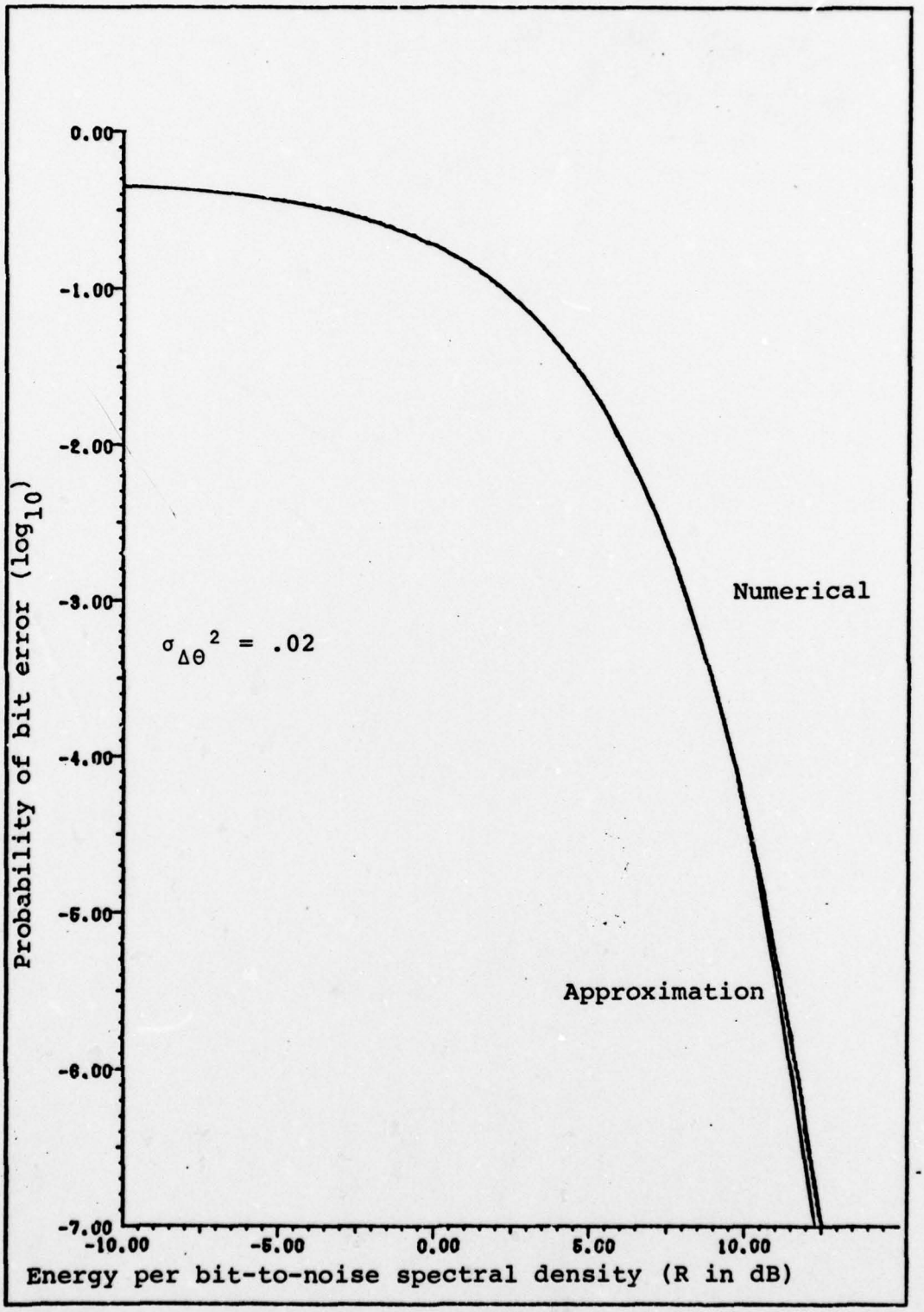

Figure 11. Numerical vs Approximate Probability of Error $\sigma_{\Delta\theta}^2$ = .02.

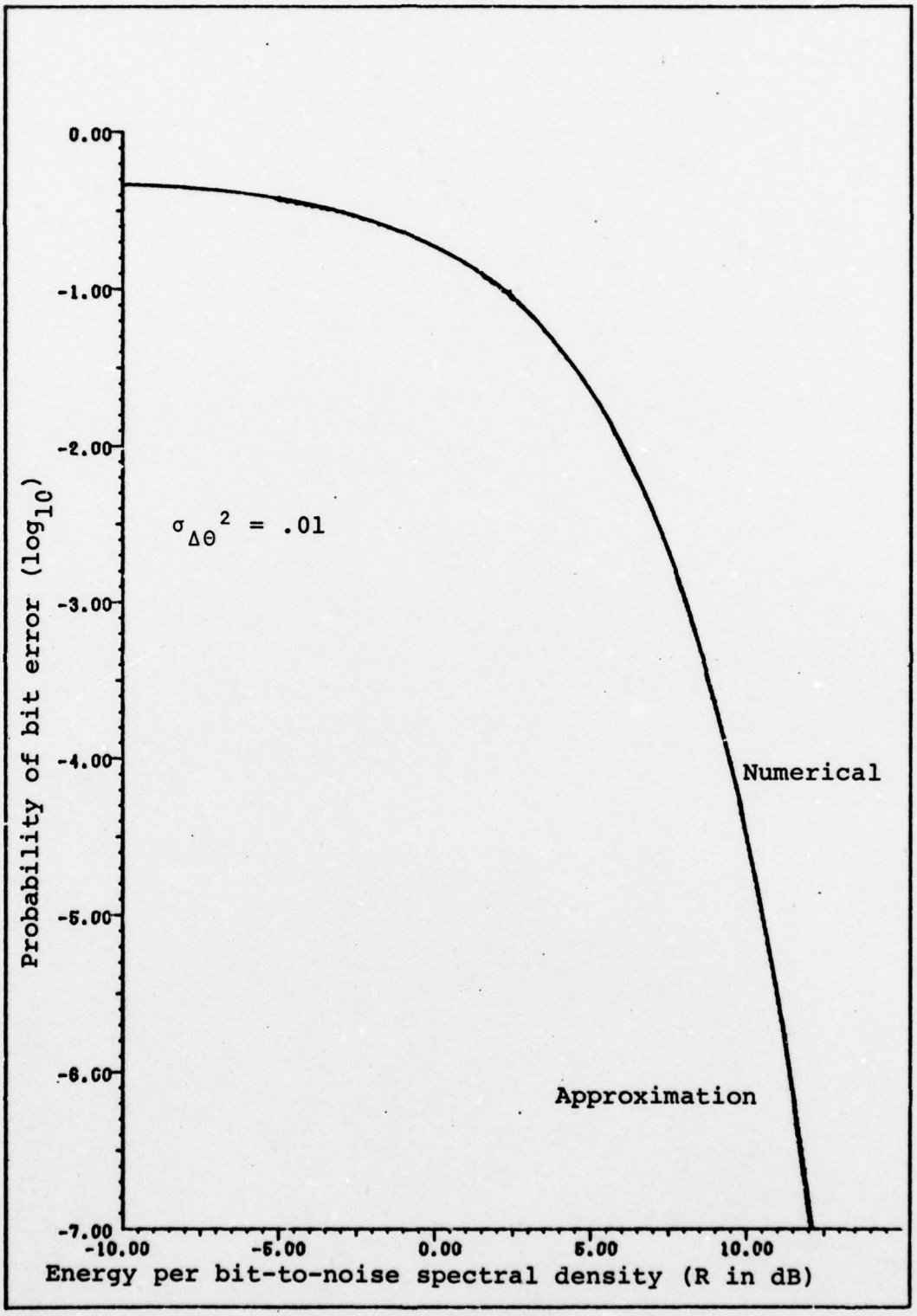

Figure 12. Numerical vs Approximate Probability of Error $\sigma_{\Delta\theta}^2 = .01$.

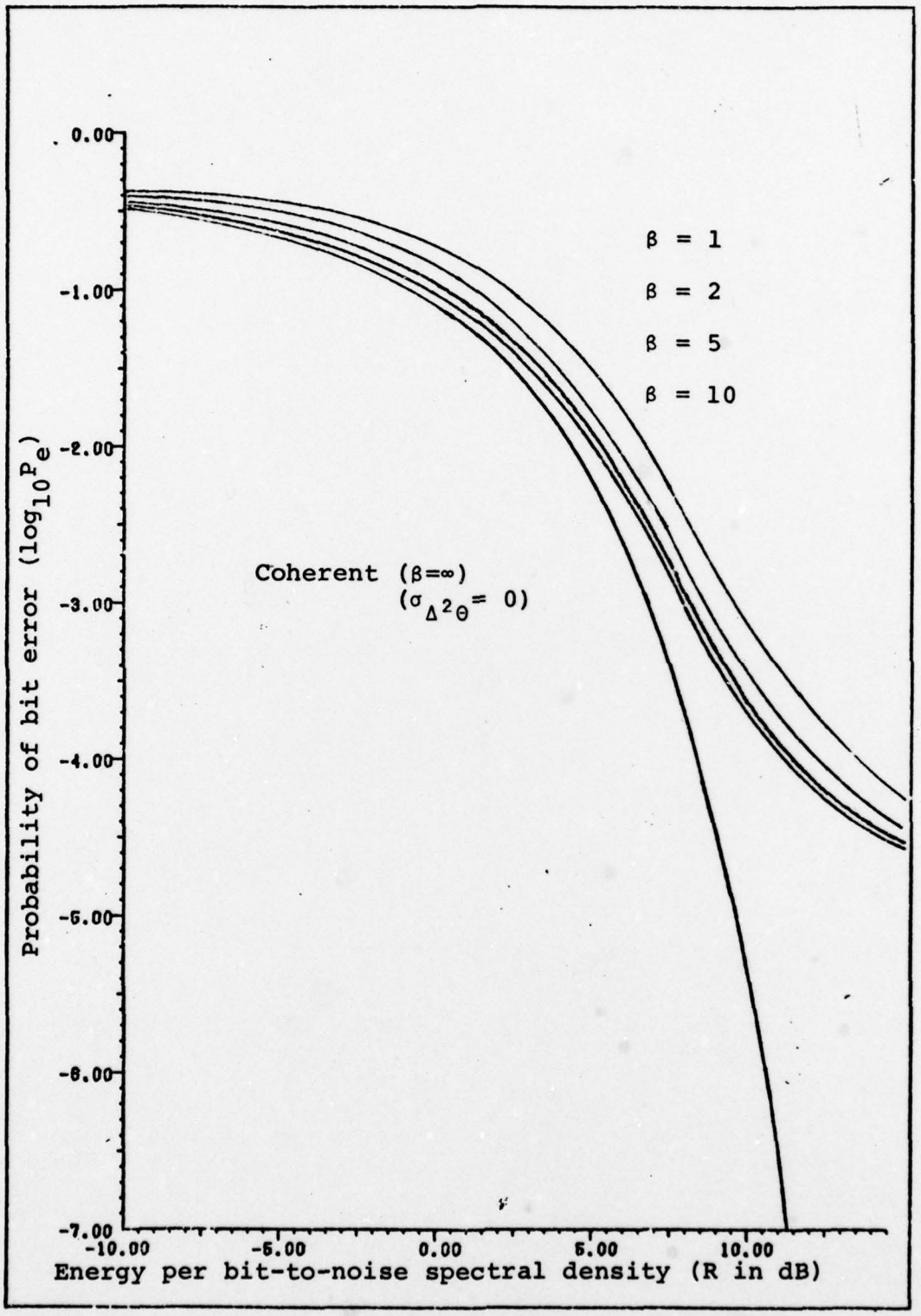

Figure 13. Error performance with $\sigma^2_{\Delta\Theta}$ = .1 and various values of β .

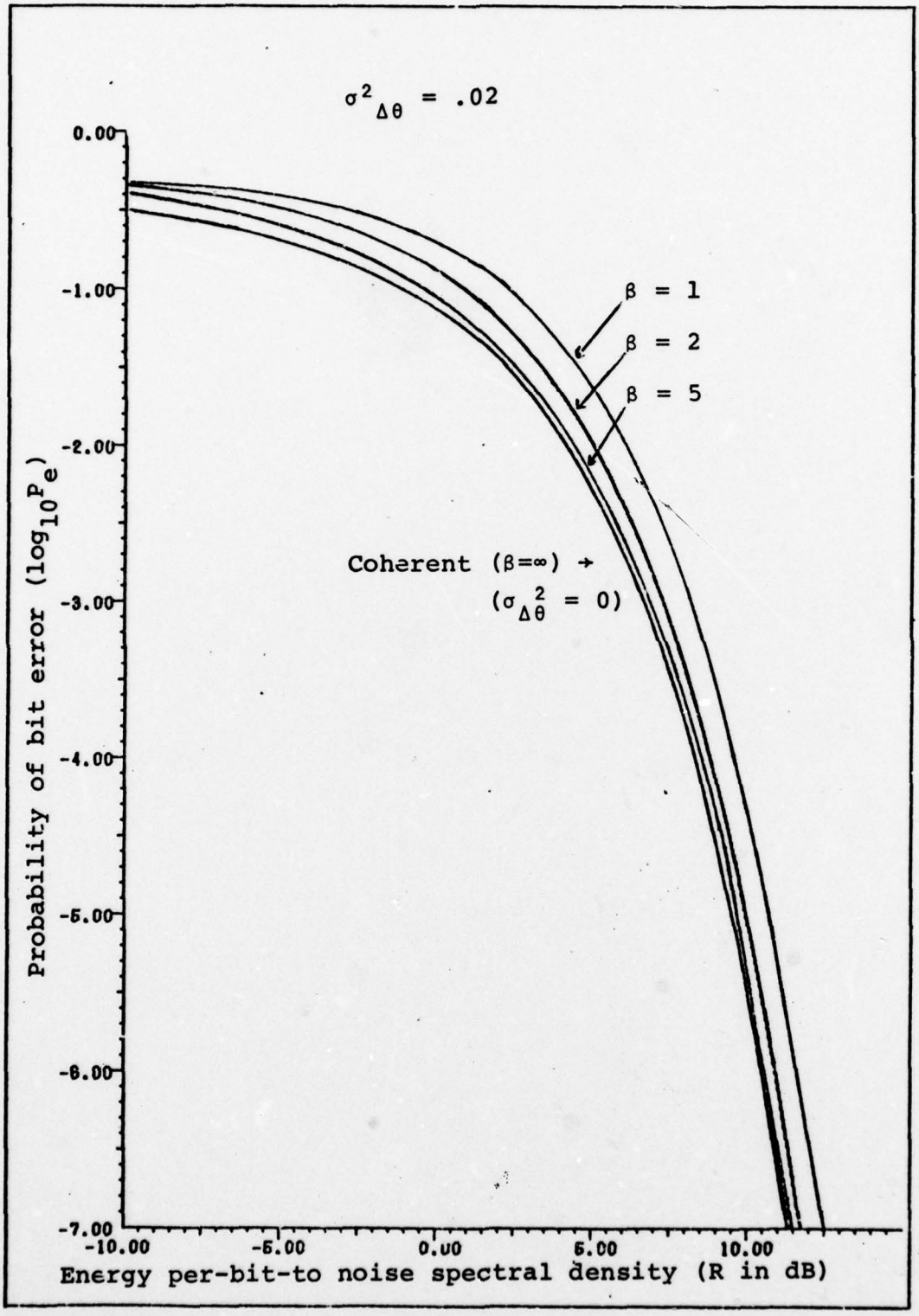

Figure 14. Error performance with $\sigma^2_{\Delta\theta}$ = .02 and various values of β .

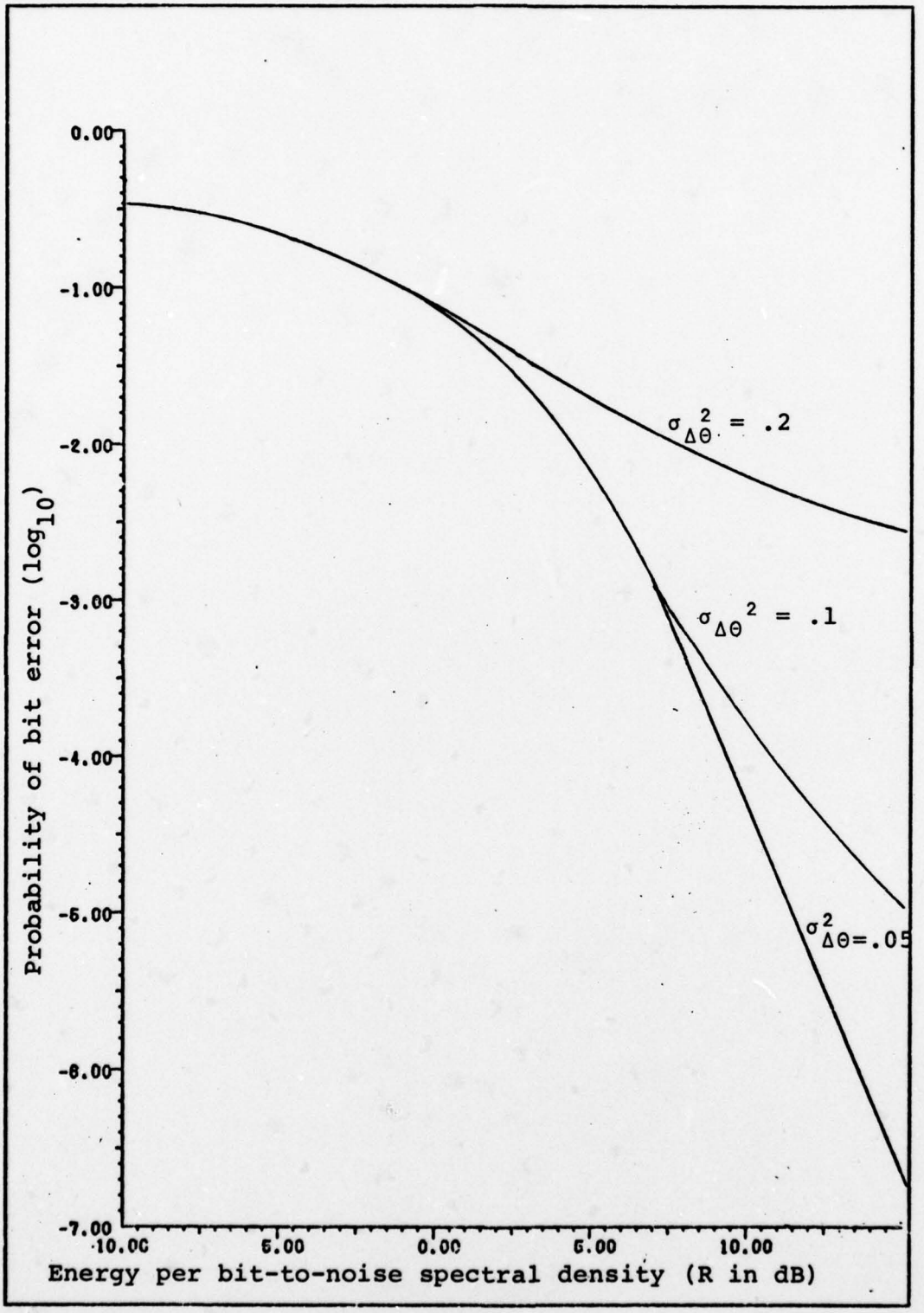

Figure 15. Error Performance with $\beta = \infty$

20dB or greater. The impact of these results will be discussed in the final chapter after some special cases of the generic receiver are examined.

Special Configuration of the Generic Receiver. As previously mentioned, if the filters in the generic receiver are bypassed and the data feedback eliminated, the resultant receiver is the DPSK receiver of Figure 16, where Figure 16 is a redrawing of Figure 5 relabeled in terms of the components of $\bar{S}_o$ and $\bar{U}$. The vectors $\bar{S}_o$ and $\bar{U}$ for the DPSK receiver are redefined as

$$\bar{U}(k) \equiv \begin{bmatrix} I(k-1) \\ Q(k-1) \end{bmatrix} \tag{59}$$

$$\bar{S}_0(k) \equiv \begin{bmatrix} I(k) \\ Q(k) \end{bmatrix} \tag{60}$$

where

$I(k-1) = \hat{I}(k)$ of the generic receiver and $Q(k-1) = \hat{Q}(k)$ of the generic receiver for this special DPSK case. The (k-1) indicates that the k^{th} data bit was delayed T_b seconds.

The optimum decision from Eq (43) is:

$$I(k)\ I(k-1) + Q(k)\ Q(k-1) \underset{0}{\overset{1}{\gtrless}} 0 \tag{61}$$

The performance given $\Delta\theta$ is given by Eq (44) or (45) where $\beta = 1$ in a and b so that:

$$a = R(1-\cos\Delta\theta) \tag{62}$$

$$b = R(1+\cos\Delta\theta) \tag{63}$$

The results for the DPSK receiver when phase varies during $2\ T_b$ seconds is given by Figures 8 thru 12 for various values of $\sigma_{\Delta\theta}{}^2$. From Appendix A when $\alpha = \infty$ or $\sigma_{\Delta\theta}{}^2 = 0$ Eq (44) and (45) reduce to the DPSK benchmark results of Eq (40), as would be expected.

A possible modification of the DPSK receiver would be to estimate the value of the received vector $\overline{S}_0$ when a binary one is sent or 180° if binary zero is sent.

The optimal estimator is the maximum likelihood (ML) estimator. The ML processor is given in Figure 17. The derivation for the ML estimate of $\cos\theta(k)$ and $\sin\theta(k)$ is rather detailed, and is derived in Appendix C. The assumptions made in deriving the ML estimator are that the $\theta(k)$ phase measurements are independent and there are no a priori statistics on $\theta(k)$.

The form of $\overline{S}_0$ remains unchanged, however, $\overline{U}$ is given by:

$$\overline{U} = \begin{bmatrix} \widehat{\cos\theta(k-1)} \\ \widehat{\sin\theta(k-1)} \end{bmatrix} \tag{64}$$

where

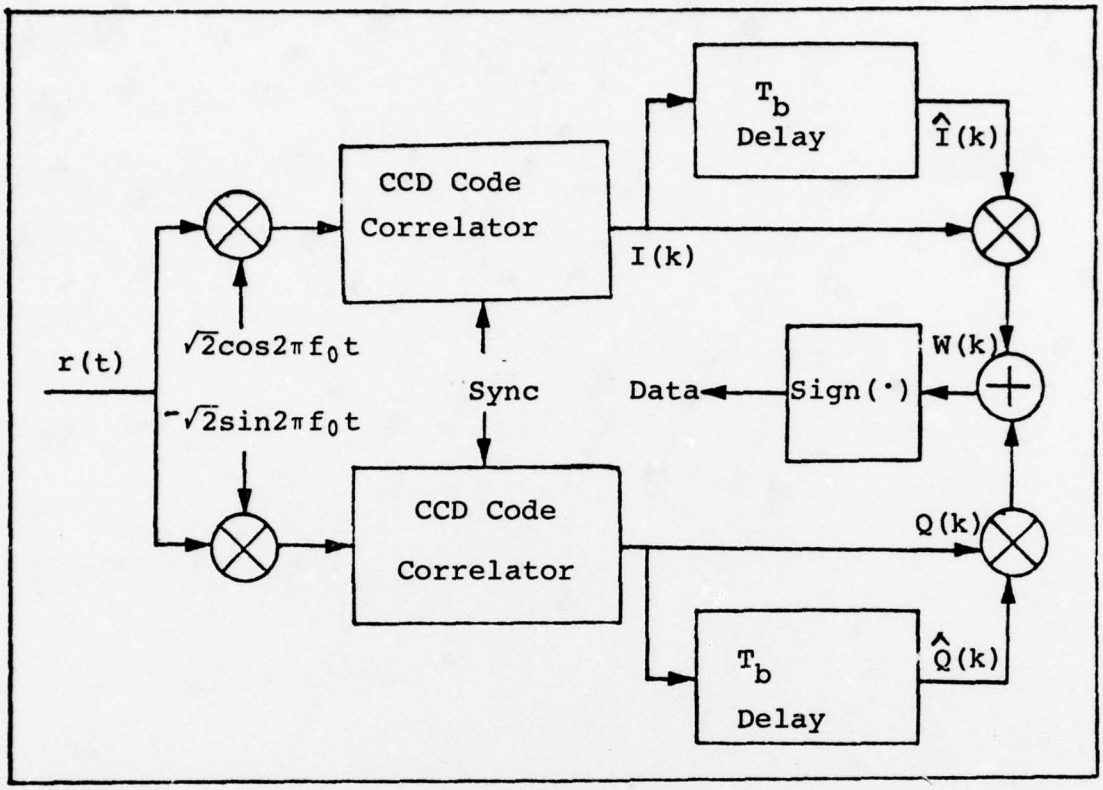

Figure 16. DPSK Case of Generic Receiver.

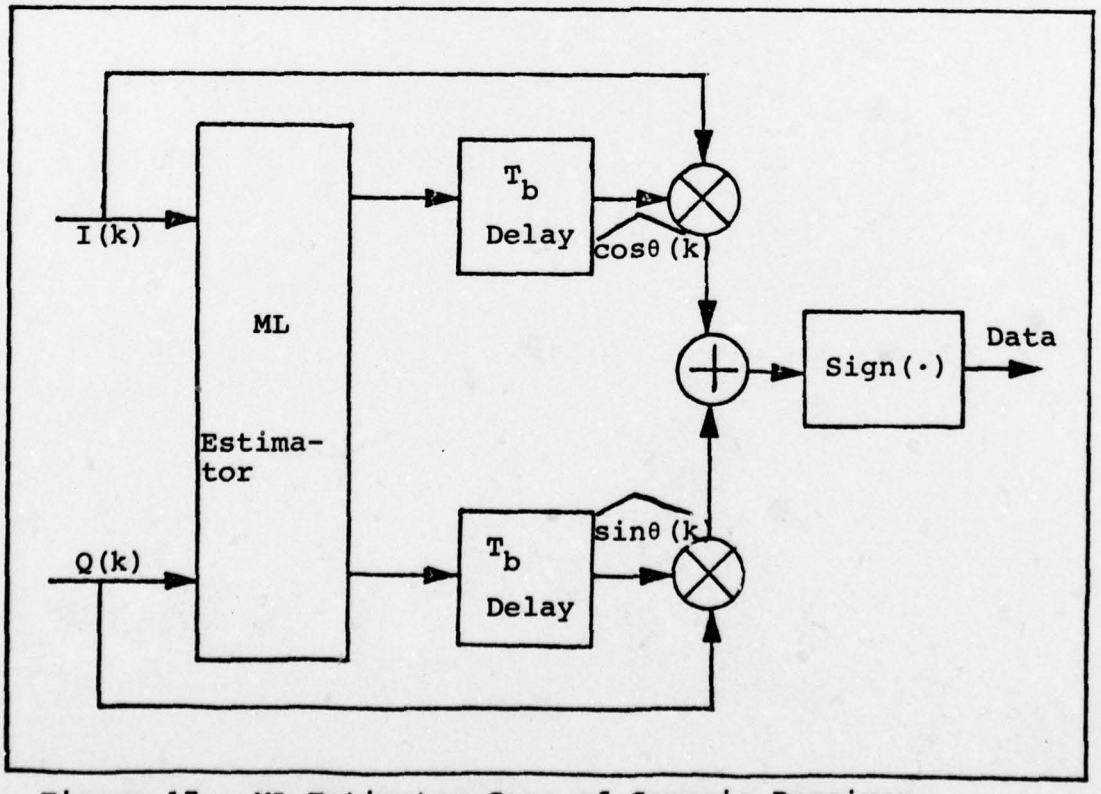

Figure 17. ML Estimator Case of Generic Receiver.

$\hat{X}$ is the ML estimate of X

The ML estimator of Appendix C merely normalizes the $\bar{U}$ vector to a unit vector and the detection scheme is equivalent to the DPSK receiver. The error performance is also equivalent to the DPSK receiver. The ML estimator proceeded by the data feedback provides a normalized output suitable for further processing such as predicting the k^{th} $\Delta\theta$ from the preceeding values. As previously mentioned, the ML estimator assumed there were no apriori statistics on $\Delta\theta$ and the $\theta(k)$ measurements were uncorrelated. The phase process $\theta(t)$ is however well defined and the correlation given by Eq (9) it is then conceivable that useful information was ignored in using the ML estimator. Perhaps a more suitable estimator is a minimum mean squared error (MMSE) or a maximum posteriori (MAP) or a predictor such as a Kalman filter. Such predictors and estimators are not the subject of this paper, however, they could possibly reduce $\sigma^2_{\Delta\theta}$ which from Figures 8 thru 12 clearly improves performance of the receiver.

Chapter IV. Conclusions and Recommendations

The significant results and recommendations for further study are addressed in this chapter.

Conclusion

The advantage of examining the generic receiver is evident in the limiting cases and by varying $\sigma_{\Delta\theta}^2$ and β . The graphs of performance, Figures 8 thru 12, show that $\sigma_{\Delta\theta}^2$ is the most sensitive parameter. When β is varied from 1 to ∞ , the performance improves slightly in the threshold region, whereas when $\sigma_{\Delta\theta}^2$ is reduced from .1 rad^2 to .05 rad^2 , the performance improved rapidly. The results indicate that the design effort in the generic receiver should be concentrated on predicting/estimating the phase quadrature to reduce $\sigma_{\Delta\theta}^2$. The apriori model for the differential phase $\Delta\theta$ is well developed therefore, it is conceivable that a Kalman filter, MAP, or MMSE could reduce $\sigma_{\Delta\theta}^2$.

The requirement that CCDs operate at baseband indicates that the generic baseband receiver is a useful approach to pursue. The CCDs are an excellent choice for code correlators because of their flexibility, however, they operate in the baseband region and require processing of the incoming signal at baseband. Because of this baseband processing restriction, the generic baseband receiver is not the optimal processor. Additionally, the performance is completely defined by $\sigma_{\Delta\theta}^2$ and β , thus simplifying performance analysis.

Recommendations

The following topics for future study are not complete, however, they represent the logical extension of this thesis.

The statistical model for the differential phase process is well defined in Chapter II. The statistics of the phase process could be exploited in the design of a Kalman filter, MAP, or MMSE predictor/estimator for the quardratures of this receiver. The effort in this approach would be to reduce $\sigma_{\Delta\theta}^2$ and increase β through prediction or estimation on the quadratures. An extension to this investigation is relaxing the restrictions on T_c over T_b and possibly introducing sub-bit processing.

The next logical step in investigation is the introduction of a more sophisticated doppler model. The receiver could possibly be aided by inertial-navigation system (INS) or other information external to the receiver to improve performance with the more sophisticated phase model.

From the recommendations, it is obvious that the analysis is not complete. This paper set up the sampled data model and developed the baseband processor. The performance did not result in a simple expression. As was mentioned in the introduction, the price for increased resistance to jamming is an increase in receiver complexity. Unfortunately, this usually translates into increased difficulty in pinpointing error performance.

Bibliography

Aurthurs, E. and H. Dym. "On the Optimum Detection of Digital Signals in the Presence of White Gaussian Noise - A Geometric Interpretation and a Study of Three Basic Data Transmission Systems," IRE Transactions on Communications Systems: 336-372, December 1962.

Brennan, L. E. and I. S. Reed. "A Recursive Method of Computing the Q Functions," IEEE Transactions on Information Theory: 312-313, April 1965.

Buss, D. D. and W. H. Bailey. "Applications of Charge Transfer Devices to Communications," Proceedings of the CCD Applications Conference: 83-90. NECC-TD-274. September 1973. (ADB 009286).

Dixon, Robert C. Spread Spectrum Techniques. New York: IEEE Press, 1976.

Downing, John J. Modulation Systems and Noise. Englewood Cliffs, NJ: Prentice-Hall, Inc., 1964.

Fleck, J. I. and E. A. Trabka. "Error Probabilities of Multiple-State Differentially Coherent Phase Shift Keyed Systems in the Presence of White Gaussian Noise." Investigation of Digital Data Communication Systems. J. G. Lawton Ed., Ithaca: Cornell Aeronautical Lab Rept No. UA-14201-S-1. January 1961.

Henery, John C. "DPSK versus FSK with Frequency Uncertainty," IEEE Transactions on Communications Technology: 814-816, December 1970.

Lindsey, W. C. and M. K. Simon. Telecommunications System Engineering. Englewood Cliffs, NJ. Prentice-Hall Inc., 1973.

Melen, R. and D. Buss. Charge Coupled Devices: Technology and Applications. New York: IEEE Press, 1977.

Papoulis, A. Probability, Random Variables, and Stochastic Processes. New York: McGraw-Hill Book Company, 1965.

Shwartz, M., W. R. Bennett, and S. Stein. Communications Systems and Techniques. New York: McGraw-Hill Book Company, 1966.

Spilker, J. J., Jr. Digital Communications by Satellite. Englewood Cliffs, NJ. Prentice-Hall, Inc. 1977.

Stein, S., "Unified Analysis of Certain Coherent and Noncoherent Binary Communications Systems." IEEE Transactions on Information Theory: 43-51, January 1964.

Stiffler, J. J., Theory of Syncronous Communications. Englewood Cliffs, NJ: Prentice-Hall, Inc., 1977.

Van Trees, H. L. Detection, Estimation, and, Modulation Theory. New York: John Wiley and Sons, 1968.

Viterbi, A. J. Principles of Coherent Communications. New York: McGraw-Hill Book Company, 1966.

Wozencraft, J. M. and I. M. Jacobs. Principles of Communications Engineering. New York: John Wiley and Sons, Inc., 1965.

Ziemer, R. E. and W. H. Tranter. Principles of Communications Systems, Modulation, and Noise. Boston: Houghton Mifflin Company, 1976.

Appendix A

The Q Function and Modified Bessel Function

This appendix contains some useful relations for the Q function and modified Bessel function (Shwartz, 1966: 585-589; and Van Trees, 1968:394-396). The definition of the Q function is given by:

$$Q(a,b) \equiv \int_b^\infty \exp\left(-\frac{a^2+x^2}{2}\right) I_0(ax)\, x\, dx \qquad \text{(A-1)}$$

where

I_0 is the modified Bessel function of order zero.

For reference, the modified Bessel function of order n is given by:

$$I_n(x) \equiv \frac{1}{2\pi} \int_0^{2\pi} \exp(\pm jn\theta)\exp(x\cos\theta)\, d\theta \qquad \text{(A-2)}$$

The limiting properties of the Q function are:

$$Q(o,b) = \exp\left(-\frac{b^2}{2}\right) \qquad \text{(A-3)}$$

$$Q(a,o) = 1 \qquad \text{(A-4)}$$

Some useful approximations of the Q function are:

$$Q(a,b) \equiv 1/2\ \text{erfc}\left(\frac{b-a}{\sqrt{2}}\right)\ b>>1,\ b>>b-a \qquad \text{(A-5)}$$

The series expansions for the Q function are given by:

$$Q(a,b) = \exp\left(-\frac{a^2+b^2}{2}\right) \sum_{n=o}^{\infty} \left(\frac{a}{b}\right)^n I_n(ab) \quad a<b \qquad \text{(A-6)}$$

$$Q(a,b) = 1-\exp\left(-\frac{a^2+b^2}{2}\right) \sum_{n=1}^{\infty} \left(\frac{b}{o}\right)^n I_n(ab) \quad b>a \qquad \text{(A-7)}$$

Three symetric and antisymetric relations for the Q function are given by:

$$1 + Q(a,b) - Q(b,a) = \frac{b^2-a^2}{b^2+a^2} \int_{\frac{a^2+b^2}{2}}^{\infty} \exp(-y) I_0\left(\frac{2aby}{a^2+b^2}\right) dy$$

$$b>a>o \qquad \text{(A-8)}$$

$$1 + Q(a,b) - Q(b,a) \simeq \operatorname{erfc}\left(\frac{b-a}{\sqrt{2}}\right) \quad b>>1, a>>1, b>>b-a>0$$

$$\text{(A-9)}$$

$$Q(a,a) = 1/2 \left[1 + I_0(a^2)\exp(-a^2)\right] \qquad \text{(A-10)}$$

The series expansion for the modified Bessel function is given by:

$$I_n(x) = \sum_{k=o}^{\infty} \frac{1}{k!(n+k)!} \left(\frac{x}{2}\right)^{n+2k} \qquad \text{(A-11)}$$

$$I_n(x) \simeq \frac{e^x}{\sqrt{2\pi x}} \quad 1 - \frac{4n^2-1}{8x} \qquad x>>1 \qquad \text{(A-13)}$$

Appendix B

A Recursive Method of Computing the Q function

The Q function can be computed recursively to a given accuracy by using the following equations (Brennan, 1965: 312-313),

$$Q(a,b) = 1 - \sum_{n=o} g(n) \cdot k(n) \qquad \text{(B-1)}$$

where:

$$g(n) - g(n-1) - \frac{1}{n!} \left(\frac{b^2}{2}\right)^n e^{-b^2/2} \qquad \text{(B-2)}$$

and:

$$k(n) = \frac{a^2}{2} \quad \frac{k(n-1)}{n} \qquad \text{(B-3)}$$

with:

$$g(o) = e^{-b^2/2} \qquad \text{(B-4)}$$

and:

$$k(o) - e^{-a^2/2} \qquad \text{(B-5)}$$

After N iterations, the error in the remaining terms is given by:

$$R_N = \sum_{N}^{\infty} g(n) \cdot k(n) \qquad \text{(B-6)}$$

A useful upper bound on R_N is given by:

$$R_N < (k(N) \cdot g(N) / (1 - (\frac{a^2 b^2}{4N^2})) \qquad \text{(B-7)}$$

for:

$$N > \frac{ab}{2} \qquad \text{(B-8)}$$

The summation in Eq (B-1) is initialized using Eqs (B-4) and (B-5), then Q is computed recursively until the remainder criteria in Eq (B-7) is met or exceeded. The series converges rapidly when $n>N$ (Brennan, 1965:313).

Appendix C

Derivation of Maximum Likelihood Estimate of Cos θ and Sin θ

The receivers in Chapter III all perform some form of the dot product to recombine the quadrature signals from the output of the correlators. One method of obtaining the projection of the received signal vector $\bar{S}_0$ onto $\bar{U}$ is to form the scalar product. The scalar product of two vectors $\bar{S}_0$ and $\bar{U}$ is:

$$\bar{S}_0 \cdot \frac{\bar{U}}{|\bar{U}|} = |\bar{S}_0| \cos \phi \qquad |\bar{U}|>0 \qquad \text{(C-1)}$$

where

$\bar{x}$ is the vector x

$|\bar{x}|$ is the magnitude of the vector

$\bar{x} \cdot \bar{y}$ is the dot product of the vector $\bar{x}$ and $\bar{y}$

ϕ is the smallest angle between $\bar{S}_0$ and $\bar{U}$

The quantity $\frac{\bar{U}}{|\bar{U}|}$ is a unit vector in the direction of $\bar{U}$. The components of $\bar{b}$ are defined as in Figure C-1 and the components of the unit vector are:

$$\frac{\bar{U}}{|\bar{U}|} = \cos\theta\bar{i} + \sin\theta\bar{j} \qquad \text{(C-2)}$$

where

θ is the angle between $\bar{U}$ and $\bar{S}_0$ direction

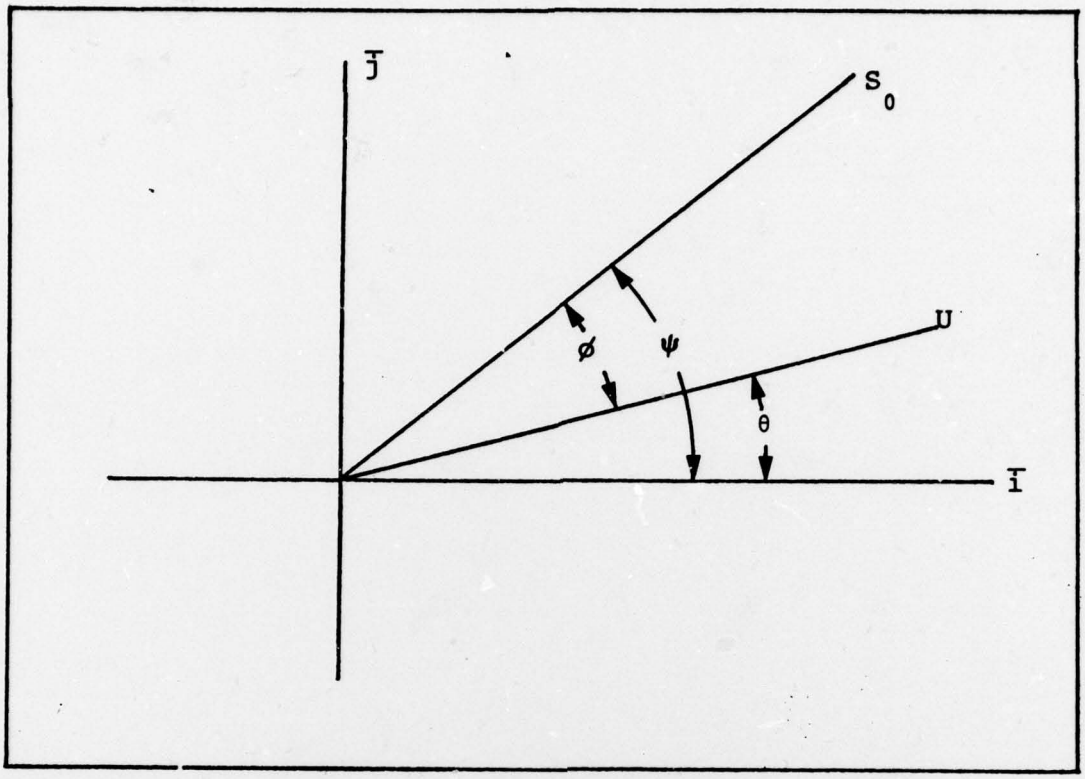

Figure C-1. Dot Product of Vectors $\bar{S}_0$ and $\bar{U}$.

$$\bar{S}_0 + \frac{\bar{U}}{|\bar{U}|} = S_{01}\cos\theta\bar{I} + S_{02}\sin\theta\bar{J} \qquad \text{(C-3)}$$

where

S_{01} is the component of $\bar{S}_0$ in the $\bar{I}$ direction

S_{02} is the component of $\bar{S}_0$ in the $\bar{J}$ direction

The components of $\bar{S}_0$ can be rewritten as:

$$S_{01} = |\bar{S}_0| \cos\Psi \qquad \text{(C-4)}$$

$$S_{02} = |\bar{S}_0| \sin\Psi \qquad \text{(C-5)}$$

Using Eqs (C-4) and (C-5) in Eq (C-3):

(C-6)

which reduces to:

$$\bar{S}_0 \cdot \frac{\bar{U}}{|\bar{U}|} = \left|\bar{S}_0\right| \cos(\Psi-\theta) \qquad \text{(C-7)}$$

But, $\Psi-\theta = \phi$ from Figure C-1 and Eq (C-7) is rewritten:

$$\bar{S}_0 \cdot \frac{\bar{U}}{|\bar{U}|} = |\bar{S}_0| \cos\phi \qquad \text{(C-8)}$$

The results in Eq (C-8) are the motivation for the determination of the $\cos\theta$ and $\sin\theta$ components of the vector $\bar{U}$. In Figure C-1, the vector $\bar{S}_0$ represents the received signal r(t) decomposed into an orthogonal vector $\bar{r}_c$ and $\bar{r}_s$ dotted with the signal vector $\bar{s}_0$. The $\bar{U}$ vector is defined in a similar manner except it dots the $\bar{r}_c$ and $\bar{r}_s$ vector with the $\bar{u}$ vector. The closer the estimate of $\cos\theta$ and $\sin\theta$ is to $\cos\theta$ and $\sin\Psi$ the more closely the receiver approaches coherent operation with $\theta = \Psi$ the coherent result.

The maximum likelihood (ML) estimate of $\cos\theta$ and $\sin\theta$ given the statistics of $\bar{U}$ is the best estimate of $\cos\theta$ and $\sin\theta$ (Van Trees, 1968:160). The ML estimate is found by solving the equation for the sufficient condition:

$$\left.\frac{d \ln f(x|y)}{dy}\right|_{y=y_{ML}} = 0 \qquad \text{(C-9)}$$

where

d is the partial derivative operator

ln(x) is the natural log of x

The output of the correlators is I(k) and Q(k) as given in Chapter II. Using the reference in Figure C-1, I(k) is in the $\bar{I}$ direction and Q(k) is in the $\bar{j}$ direction. The conditional density of I(k) and Q(k) given θ and that the noise is independent between samples is:

$$f(\bar{I},\bar{Q}|\bar{\theta}) = \prod_{k=1}^{N} \frac{1}{\sqrt{2\pi}\sigma} \exp\left\{-1/2 \frac{(I(k)-ANT_c\cos\theta(k)^2}{\sigma^2}\right\}$$
$$\cdot \prod_{k=1}^{N} \frac{1}{\sqrt{2\pi}\sigma} \exp\left\{-1/2 \frac{(Q(k)-ANT_c\sin\theta(k))^2}{\sigma^2}\right\} \qquad \text{(C-10)}$$

where

$\bar{I}$ is an NX1 vector

$\bar{Q}$ is an NX1 vector

$\bar{\theta}$ is an NX1 vector

$\prod_{k=1}^{N}$ is an N-fold multiplication of each term from k = 1 to N

σ^2 is the variance of the Gaussian variables

The data term $d(k)$ in $I(k)$ is assumed to be $d_1(k)$ so that Eq (C-10) is a valid density to use in Eq (C-9). If the phase is assumed to be independent between samples, the ML estimate for $\cos\theta(k)$ is found by solving:

$$\left.\frac{d\ln f(\bar{I},\bar{Q}|\bar{\theta})}{d\cos\theta(k)}\right|_{\cos\theta(k)=\cos\theta(k)_{ML}} = 0 \qquad \text{(C-11)}$$

Then

$$\frac{d\ln f(\bar{I},\bar{Q}|\bar{\theta})}{d\cos\theta(k)} = \frac{1}{\sigma^2}\left[I(k)ANT_c - \frac{Q(k)ANT_c\cos\theta(k)}{\sqrt{1-\cos^2\theta(k)}}\right] \qquad \text{(C-12)}$$

Setting Eq (C-13) equal to zero and solving for yields:

$$\widehat{\cos\theta(k)}_{ML} = \frac{I(k)}{\sqrt{I(k)^2 + Q(k)^2}} \qquad \text{(C-13)}$$

The results for $\sin\theta(k)_{ML}$ are derived in a similar fashion and the result is:

$$\widehat{\sin\theta(k)}_{ML} = \frac{Q(k)}{\sqrt{I(k)^2 + Q(k)^2}} \qquad \text{(C-14)}$$

The results in Eqs (C-14) and (C-15) seem intuitive from the operation in Eq (C-2). Additionally, the estimates are the ML estimates for $\cos\theta(k)$ and $\sin\theta(k)$. The assumptions for Eqs (C-14) and (C-15) to be valid are that the phase $\theta(k)$ is constant over a bit interval T_b . Also, the phase $\theta(k)$ is independent of the previous phase sample.

The Cramer-Rao (C-R) bound of the estimates of the $\cos\theta$ and $\sin\theta$ give an indication of the variance of the lower bound on the estimate. The C-R bound is given by (Van Trees, 1968:437):

$$\left\{ - E \left[\frac{d^2 f(x|y)}{dy^2} \right] \right\}^{-1} \qquad \text{(C-15)}$$

where

$E[x]$ is the expected value of x

d^2 is the second partial derivative

The first partial derivative of $\cos\theta$ is the right side of Eq (C-13) so taking the partial derivative of Eq (C-13) and letting $\mathfrak{z} = \cos\theta(k)$ and $\sin\theta(k) = \sqrt{1-\mathfrak{z}^2}$ yields

$$\frac{d^2 f(\bar{I},\bar{Q}|\bar{\theta})}{d\cos\theta(k)^2} = \frac{Q(k) A N T_c}{\sigma^2 (1-\mathfrak{z})^2} \left(\sqrt{1-\mathfrak{z}^2} + \frac{\mathfrak{z}^2}{\sqrt{1-\mathfrak{z}^2}} \right) \qquad \text{(C-16)}$$

Taking the expected value of Eq (C-17) and inverting:

$$C\text{-}R_{\widehat{\cos\theta(k)}_{ML}} = \frac{N_0 \sin^2\theta(k)}{E_b} \qquad \text{(C-17)}$$

where

E_b is given as the energy per bit from Chapter II.

The C-R bounds can be rewritten:

$$C\text{-}R_{\widehat{\cos\theta(k)}_{ML}} = R \sin^2 \theta(k) \qquad \text{(C-19)}$$

$$C\text{-}R_{\widehat{\sin\theta(k)}_{ML}} = R \cos^2 \theta(k) \qquad \text{(C-20)}$$

The C-R bounds for $\widehat{\cos\theta(k)}_{ML}$ and $\widehat{\sin\theta(k)}_{ML}$ are a function of $\theta(k)$. Unfortunately, as in the case of $\theta(k) = 0$ radians, the C-R bound for $\cos\theta(k)_{ML}$ is zero, which underbounds all estimates. The C-R bound in this case does not give a tight bound on the variance of the expected performance. This fact does not exclude the use of Eqs (C-14) and (C-15) as the optimal estimates it is just that tight bounds on performance cannot be determined using the C-R bounding technique.

Vita

John Gary Pennett was born on 23 April 1952 in Philadelphia, Pennsylvania. He was graduated from Kailua High School in Kailua, Hawaii in 1970. He attended the United States Air Force Academy from which he received the degree of Bachelor of Science in Electrical Engineering and was commissioned in the USAF in June 1974. He completed the Communications Electronics Engineer course at Keesler AFB, Mississippi in March 1975. He was assigned to Pacific Communications Area Hq at Hickam AFB Hawaii. While at PCA Hq he was a test director in the AFCS Scope Creek communications evaluation project. In June 1977 he entered the School of Engineering, Air Force Institute of Technology.

Permanent Address: 49 Clinton Street
Rossiter, Pennsylvania 15772

UNCLASSIFIED

SECURITY CLASSIFICATION OF THIS PAGE (When Data Entered)

REPORT DOCUMENTATION PAGE	READ INSTRUCTIONS BEFORE COMPLETING FORM
1. REPORT NUMBER (14) AFIT/GE/EE/78-36	2. GOVT ACCESSION NO. (9)	3. RECIPIENT'S CATALOG NUMBER: Master's thesis
4. TITLE (and Subtitle) (6) Performance of a Phase Comparison Spread Spectrum Receiver.	5. TYPE OF REPORT & PERIOD COVERED: MS Thesis
	6. PERFORMING ORG. REPORT NUMBER
7. AUTHOR(s) (10) JOHN Gary PENNETT, CAPT, USAF	8. CONTRACT OR GRANT NUMBER(s) (12) 73p.
9. PERFORMING ORGANIZATION NAME AND ADDRESS: Air Force Institute of Technology (AFIT/EN) Wright-Patterson AFB, OH 45433	10. PROGRAM ELEMENT, PROJECT, TASK AREA & WORK UNIT NUMBERS (16) 2277
11. CONTROLLING OFFICE NAME AND ADDRESS: Rome Air Development Center/DCID Griffis AFB, NY 13441 (11)	12. REPORT DATE: Dec 1978
	13. NUMBER OF PAGES
14. MONITORING AGENCY NAME & ADDRESS(if different from Controlling Office)	15. SECURITY CLASS. (of this report): Unclassified
	15a. DECLASSIFICATION/DOWNGRADING SCHEDULE

16. DISTRIBUTION STATEMENT (of this Report)

Approved for public release; distribution unlimited.

17. DISTRIBUTION STATEMENT (of the abstract entered in Block 20, if different from Report)

18. SUPPLEMENTARY NOTES

Approved for public release; IAW AFR 190-17

J. P. Hipps, Major, USAF
Director of Information 1-23-79

19. KEY WORDS (Continue on reverse side if necessary and identify by block number)

Charge Coupled Devices (CCD)
Spread Spectrum Communications
Antijam Communications
Phase Shift Keyed (PSK)
Digital Communications

20. ABSTRACT (Continue on reverse side if necessary and identify by block number)

A phase comparison receiver is implemented at baseband with charge-coupled device (CCD) correlators as matched filters. The received signal is a pseudo-noise (PN) phase coded spread spectrum waveform. The effects of doppler-induced frequency instabilities on the probability of error performance is examined with the differential phase modeled as a Gaussian process. Numerical results are presented and when the variance is greater than .1 radians^2 the performance degrades rapidly. An analytic approximation is given for probability of error for specific cases and is useful for small values of variance and low signal-to-

next page

DD FORM 1 JAN 73 1473 EDITION OF 1 NOV 65 IS OBSOLETE

UNCLASSIFIED

SECURITY CLASSIFICATION OF THIS PAGE (When Data Entered)

radians-squared 012 225

noise ratios. In the limit when the variance approaches zero, the receiver performance expression is equivalent to the differentially coherent phase shift keyed (DPSK) receiver. If the reference is perfect in addition to the zero phase variance the performance is the same as a phase coherent receiver with a perfect reference.